THE ASTROPHYSICAL JOURNAL, 414:41–56, 1993 September 1

SHARP EDGES TO NEUTRAL HYDROGEN DISKS IN GALAXIES AND THE EXTRAGALACTIC RADIATION FIELD

PHILIP MALONEY[1]
Sterrewacht Leiden and NASA Ames Research Center
Received 1992 April 7; accepted 1993 March 9

ABSTRACT

Recent observations of the late-type spiral galaxy NGC 3198 show that the extended atomic hydrogen distribution in this galaxy is sharply truncated at a neutral hydrogen column density of $N_{\rm H\,I} \approx 5 \times 10^{19}$ cm^{-2} (van Gorkom et al. 1993). In this paper I show that this cutoff can be reasonably explained as the result of photoionization of the gas by the extragalactic radiation field. I treat the gaseous disk in plane-parallel geometry, with the vertical equilibrium explicitly calculated for a composite disk/halo model; the gas is assumed to be smoothly distributed and isothermal, with $T \sim 10^4$ K. The extragalactic radiation field is taken to be a power law between the Lyman limit and the observed value at 1.5 keV; the actual intensity at the Lyman limit is a free parameter. Models calculated for a range of velocity dispersions and ionizing photon fluxes show similar behavior, with a characteristic column density $N_{\rm cr} \sim$ a few times 10^{19} cm^{-2} at which the ionization fraction sharply increases. This result is not significantly affected by halo eccentricity, but does depend on the clumpiness of the gas. Specific application to NGC 3198 shows that the total hydrogen distribution may be nearly axisymmetric, and that the atomic hydrogen at large radii is not significantly clumped into clouds. The column density at which this transition occurs is not very sensitive to galaxy mass or halo parameters, changing by only a factor of $\sim$3 as the halo surface density Σ_h is varied by a factor of $\sim$30. The numerical results are in good agreement with an analytic estimate of the critical column density; the analytic result shows that $N_{\rm cr} \propto [\phi_{i,\rm ex}\,\sigma_{zz}\,V_{\rm A}/\Sigma_h]^{1/2}$, where $V_{\rm A}$ is the halo asymptotic velocity, σ_{zz} is the gas vertical velocity dispersion, and $\phi_{i,\rm ex}$ is the extragalactic ionizing photon flux. Because of the insensitivity to galaxy parameters, this model predicts that all disk galaxies will show sharp edges to their neutral hydrogen distributions at similar column densities, as first discussed by Bochkarev & Sunyaev (1977). It also predicts that objects with atomic hydrogen surface densities below this critical value will be mostly ionized and hence undetectable in the 21 cm line. If the observed H I cutoffs are due to photoionization, the extragalactic ionizing photon flux in the energy range $h\nu = 13.6 \sim 200$ eV must be $5 \times 10^3 \lesssim \phi_{i,\rm ex} \lesssim 5 \times 10^4$ photons cm^{-2} s^{-1}. The emission measure EM of ionized gas at large radii is generally too small to be detectable by emission in Hα at present. Strict limits on or eventual measurement of EM(R) and determination of the neutral gas velocity dispersion will allow a more precise determination of $\phi_{i,\rm ex}$.

Subject headings: dark matter — diffuse radiation — galaxies: individual (NGC 3198) — galaxies: ISM — galaxies: kinematics and dynamics

1. INTRODUCTION

Neutral atomic hydrogen is the most easily observed constituent of the interstellar medium in galaxies. With the advent of sensitive interferometers such as the Westerbork Synthesis Radio Telescope (WSRT) and the Very Large Array (VLA),[2] observations in the 21 cm line have been used not only to study the interstellar medium in galaxies but also as a probe of galactic kinematics and dynamics. Studies using the WSRT and VLA have shown that neutral hydrogen is typically extended beyond the optical disk in noncluster spirals, with $R_{\rm H\,I}/R_{\rm Ho} \sim$ 1–2, where $R_{\rm Ho}$ is the Holmberg radius (typically occurring at 4–5 disk scale lengths) and $R_{\rm H\,I}$ is the galaxy radius at a characteristic column density $N_{\rm H\,I} \sim 10^{20}$ cm^{-2} (Bosma 1981; Wevers 1984; Sancisi 1987).

The neutral hydrogen distribution in the Sc spiral NGC 3198 was studied using the WSRT by van Albada et al. (1985). With a column density sensitivity of $N_{\rm H\,I} \approx 5 \times 10^{19}$ cm^{-2}, they found that the neutral hydrogen extended to $R \approx 30$ kpc (for a distance $D = 9.4$ Mpc, assuming $H_0 = 75$ km s^{-1} Mpc^{-1}). This corresponds to 11 scale lengths of the stellar disk, whose light distribution is well described by an exponential; any bulge is negligible. The rotation curve of NGC 3198 rises to $V \approx 150$ km s^{-1} within 5 kpc and remains flat (to within a few km s^{-1}) out to the last measured point. The galaxy is inclined to the plane of the sky by $i \approx 72°$, so that the rotation curve is well determined. Beyond $R \gtrsim 15$ kpc, the neutral atomic hydrogen distribution is reasonably well described by an exponential with a scale length of $\sim$9 kpc.

The actual extent—and hence total mass—of dark matter halos around disk galaxies is still generally unknown. To address this question, van Gorkom et al. (1993) reobserved NGC 3198 using the VLA, integrating for 100 hr in order to improve their sensitivity by an order of magnitude, to $N_{\rm H\,I} \approx 4 \times 10^{18}$ cm^{-2}. If the neutral hydrogen column density continued to decline as an exponential with an e-folding length of $\sim$9 kpc, van Gorkom et al. could have expected to measure emission to $R \sim 56$ kpc. Instead, they found that to within their beam size, $1' \approx 2.7$ kpc, the 5×10^{19} cm^{-2} and 4×10^{18}

[1] Present address: Joint Institute for Laboratory Astrophysics, Campus Box 440, University of Colorado, Boulder, CO 80309.

[2] The VLA is a facility of the National Radio Astronomy Observatory, which is operated by Associated Universities, Inc., under contract with the National Science Foundation.

cm^{-2} levels are spatially coincident: the neutral hydrogen column density drops by an order of magnitude in less than 3 kpc (van Gorkom 1991). This result holds at all azimuthal angles around the galaxy, which rules out the possibility that it is a projection effect cause by, e.g., a warp in the neutral hydrogen layer. Thus the neutral hydrogen distribution is very sharply truncated, with $\Delta R/R \lesssim 0.1$.

Does this cutoff represent a sharp physical edge to the gas distribution in this galaxy, or merely reflect a change in the physical state of the gas? In this paper, I suggest that the sudden truncation results from the photoionization of the neutral gas by the extragalactic radiation field. At such large distances from the optical disk of the galaxy it is very unlikely that any source of ionization from within the galaxy can be significant. As with other photoionization processes, one expects that there will be a fairly abrupt transition in the gas from mostly neutral to mostly ionized, with the transition occurring at some critical column density, N_c. Here the problem is essentially an inverse Strömgren region problem, with ionizing photons incident on the exterior of a gaseous disk. A rough estimate as to the feasibility of this model can be made as follows: consider an atomic hydrogen layer of fixed thickness and constant density n. A flux of ionizing photons with $\phi_{i,ex}$ photons cm^{-2} s^{-1} is incident on both sides of the gas layer. Then there is a critical column density,

$$N_c \approx \frac{2\phi_{i,ex}}{\alpha_{rec} n} \tag{1}$$

(where α_{rec} is the hydrogen recombination coefficient), below which the column recombination rate $\alpha_{rec} n N_c$ is too small to balance the ionizing photon flux $2\phi_{i,ex}$. Hence gas column densities below N_c will be mostly ionized and column densities above N_c will be mostly neutral. Numerically, using $\alpha_B = 2.6 \times 10^{-13}$ cm^3 s^{-1} for α_{rec}, appropriate for $T_e \sim 10^4$ K gas,

$$N_c = 7.7 \times 10^{18} \frac{(\phi_{i,ex}/10^4)}{(n/10^{-2})} \text{ cm}^{-2}, \tag{2}$$

which is of the right order of magnitude to explain the NGC 3198 result. (Gas number densities $n \sim 10^{-3}$–10^{-2} cm^{-3} are typical of the midplane values; see § 3. Estimates for $\phi_{i,ex}$ are discussed in § 2.) An accurate estimate of this critical column density and application of this model to NGC 3198 requires a more careful treatment of the ionization equilibrium and the vertical distribution and structure of the gas at large radii in galaxies. The remainder of this paper presents a detailed treatment of this problem. The model for calculating the photoionization equilibrium is presented in § 2. Since the recombination rate in the gas is proportional to n^2 while the photoionization rate is proportional to n, the gas density distribution is important in determining the ionization state; in § 3 the vertical distribution of gas in a galactic potential is discussed. An improved analytic estimate for N_c and scaling relations are derived in § 4. Results for NGC 3198 and other galaxies are presented in § 5. The implications are discussed in § 6, and a summary of the results is presented in § 7.

The idea that photoionization of neutral hydrogen in galaxies by the extragalactic background might be important has a fairly long history. Sunyaev (1969) argued that observations showing neutral hydrogen column densities of $N_{HI} \sim 10^{20}$ around nearby galaxies such as M31 ruled out the existence of a hot ($T \sim 10^6$ K) intergalactic medium with a density close to the critical ($\Omega = 1$) density, since bremsstrahlung from the IGM would ionize the hydrogen. However, Felten & Bergeron (1969) showed that Sunyaev's argument was incorrect, using the critical column density argument that I have outlined above to show that (for $N_H > N_c$) hydrogen disks in galaxies would merely develop ionized halos around a neutral core. Silk (1971) studied the formation of the ionized boundary layer in more detail, while Hill (1974) self-consistently solved for the hydrogen column density and the extragalactic ionizing flux in the solar neighborhood, for assumed Gaussian or exponential gas vertical distributions. In an important paper, Bochkarev & Sunyaev (1977) carried out calculations similar to those of Hill, but specifically examined the question of a sharp cutoff to the neutral hydrogen distribution at large radii in galaxies, emphasizing both that a cutoff is the expected behavior and that observations of such an effect can be used to estimate the extragalactic ionizing photon flux. Silk & Sunyaev (1976) summarized the above work and reiterated the prediction of Bochkarev & Sunyaev of a sharp cutoff to the 21 cm emission. Here I present results for a wider range of parameters and more realistic galaxy models than were considered by Bochkarev & Sunyaev and treat the gas vertical distribution more accurately. I also discuss how the cutoff column density will vary as a function of galaxy parameters, and present scaling relations for the variation of N_c with $\phi_{i,ex}$, σ_{zz} and galaxy mass parameters. Preliminary results from this work were presented in Maloney (1990).

2. IONIZATION EQUILIBRIUM

The gas disk is modeled as a plane-parallel slab, with an isotropic extragalactic radiation field incident upon it. At any given depth within the gas layer, there will be two contributions to the ionizing photon flux: the attenuated direct radiation field, and the diffuse ionizing field produced by recombinations within the gas layer. The method used here to calculate the ionization equilibrium throughout the gas layer is essentially that of Williams (1967): after specification of the gas vertical (Z) distribution, the gas layer is divided up into a number of plane-parallel zones, each of which is assumed to be uniform. The source functions are assumed to be constant within each zone.

2.1. *Direct Component*

The extragalactic background radiation field is incident on both sides of the gas layer. Assuming that the disk is optically thick at frequency ν (so that the irradiation is effectively one-sided), the mean intensity due to the incident radiation at a normal optical depth t_ν into the gas layer is

$$J_\nu^e = \tfrac{1}{2} \int_{-1}^{0} I_\nu^0 e^{t_\nu/\mu} d\mu$$
$$= \tfrac{1}{2} I_\nu^0 E_2(t_\nu) \tag{3}$$

where μ is the cosine of the angle from the normal to the layer, I_ν^0 is the incident intensity of radiation, and $E_2(x)$ is the second exponential integral. The assumption of one-sidedness is explicitly checked as a function of frequency and corrected, if necessary; it will always break down at photon energies that are high enough that the entire gas layer is optically thin, but these photons will also contribute very little to the ionization.

X-ray observations above 1 keV show an isotropic component, which is assumed to be extragalactic. The background is probably produced by discrete sources such as AGNs

(Mather et al. 1990), but the precise nature of the background is not important in this context. Following Fransson & Chevalier (1985), I have assumed that the extragalactic radiation field is a power law between the Lyman limit and the observed X-ray value at 1.5 keV (Schwarz 1979). The actual intensity at the Lyman limit, $I_{\rm Ly}$, is a free parameter, normalized for convenience to the value $I(13.6\ {\rm eV}) = 4.0 \times 10^{-23}$ ergs cm^{-2} s^{-1} Hz^{-1} sr^{-1} suggested by Sargent et al. (1979) as the intensity at redshift $z = 0$ due to QSOs. The spectral index of the ionizing radiation field is then given by $\alpha = 1.45 + 0.490 \log (I_{\rm Ly})$ ($I_\nu \propto \nu^{-\alpha}$). The flux of ionizing photons is then $\phi_{i,{\rm ex}} = 7.6 \times 10^4\ I_{\rm Ly}/\alpha$ photons cm^{-2} s^{-1} for irradiation from 4π sr; for one-sided illumination the normally incident photon flux is $1.9 \times 10^4\ I_{\rm Ly}/\alpha$ photons cm^{-2} s^{-1}.

At present there are only upper limits to the extragalactic ionizing photon flux. Searches for Hα emission from high-velocity clouds (Reynolds 1987; Kutyrev & Reynolds 1989; Songaila, Bryant, & Cowie 1989), the intergalactic H I cloud in Leo (Reynolds et al. 1986), and the H I cloud associated with the QSO/galaxy pair 3C 232/NGC 3067 (Stocke et al. 1991) have yielded upper limits in the range $\phi_{i,{\rm ex}} \sim 10^4$–$10^5$ photons cm^{-2} s^{-1}. The contribution from QSOs provides a lower limit to the $z = 0$ ionizing photon flux; throughout this paper I will take a minimum value of $I_{\rm Ly} = 1$ and assume a maximum value $I_{\rm Ly} \lesssim 10$.

Since the incident radiation field is a power law, the usual Strömgren approximation will also break down: since soft X-ray photons penetrate to much greater depths than photons not far above the Lyman limit, the transition from highly ionized to neutral will not be sharp. Direct ionization by soft X-rays will also produce energetic primary photoelectrons leading to secondary ionizations (Shull & van Steenberg 1985). At the low densities and relatively low temperatures ($T_e \lesssim$ 20,000 K) of interest here, collisional ionization by thermal electrons will be unimportant relative to photoionization and has been ignored.

2.2. *Diffuse Component*

The ionizing radiation field also has a diffuse component, due to recombination within the gas layer. If a zone at depth Z has normal optical thickness T_ν, the emergent intensity at an angle $\cos^{-1}(\mu)$ is $I_\nu^d = S_\nu(Z)(1 - e^{-T_\nu/\mu})$, where $S_\nu(Z)$ is the zone source function. The contribution from this zone to the diffuse intensity a normal optical depth t_ν away is $I_\nu^d = S_\nu(Z)e^{-t_\nu/\mu}(1 - e^{-T_\nu/\mu})$, so the mean diffuse intensity from this zone to a layer a normal optical depth t_ν away is

$$J_\nu^d = \tfrac{1}{2}S_\nu(Z)\int_0^1 [e^{-t_\nu/\mu} - e^{-(t_\nu + T_\nu)/\mu}]d\mu$$
$$= \tfrac{1}{2}S_\nu(Z)[E_2(t_\nu) - E_2(t_\nu + T_\nu)] \quad (4)$$

which is easily evaluated.

The diffuse hydrogen-ionizing radiation field has contributions from

1. Recombinations to the ground states of H, He, and He$^+$.
2. He resonance-line emission ($2^3S \rightarrow 1^1S$ at 19.8 eV and $2^1P \rightarrow 1^1S$ at 21.3 eV).
3. He two-photon ($2^1S \rightarrow 1^1S$) emission; the sum of the emitted photon energies is 20.6 eV.
4. He$^+$ Lyα emission ($2^2P \rightarrow 1^2S$) at 40.7 eV.
5. He$^+$ Balmer continuum emission, with $E \geq 13.6$ eV.
6. He$^+$ 2-photon emission ($2^2S \rightarrow 1^1S$), for which the sum of the emitted photon energies is 40.7 eV.

In the presence of a power-law radiation field, the presence of helium can be very important for the hydrogen ionization equilibrium (Hill 1974), since He and He$^+$ are ionized by photons with energies $E \geq 24.6$ eV and $E \geq 54.4$ eV, respectively, where the hydrogen cross section for photoionization is small, while the recombination radiation from He and He$^+$ can ionize hydrogen. Thus helium acts to degrade soft X-ray, He-ionizing photons into ultraviolet, H-ionizing photons. At $T_e = 10^4$ K, 0.77 of the excited-state recombinations of He are to triplet levels, and 0.23 are to singlet levels (Osterbrock 1988). Essentially all of the captures to triplet levels lead to population of 2^3S, which is highly metastable but can decay via a forbidden-line photon at 19.8 eV. At the densities of interest here (see § 3) the rates of collisional transitions to the singlet 2^1S and 2^1P levels are negligible compared to the 19.8 eV photon emission rate. It will be assumed that all recaptures to the triplet levels produce 19.8 eV photons. Of the recombinations to the singlet levels, $\sim\frac{2}{3}$ lead to population of 2^1P while the remainder populate 2^1S. Virtually all He atoms exit the 2^1P level via emission of a 21.3 eV photon: the relative probability of decay instead to 2^1S with emission of a 2.2 μm photon is only $\sim 10^{-3}$ (Osterbrock 1988) and will be ignored. He atoms in the 2^1S level decay via two-photon emission. For He$^+$, some fraction of the excited-state recombinations will populate the 2^2P state, while the remainder end up in the 2^2S state. At $T_e = 10^4$ K, the fraction that arrive in the 2^2P state is 0.715 (Hummer & Seaton 1964). These atoms decay via emission of an He$^+$ Lyα photon at 40.7 eV. The He$^+$ atoms in the 2^2S state decay through two-photon emission; $\sim$0.71 of these photons are hydrogen-ionizing. Radiative transfer in the very optically thick He and He$^+$ Lyα lines is treated using the escape probability formalism of Elitzur & Netzer (1985); since this is a local approximation, the effect of the recombination radiation from different zones on one another is not treated for the resonance lines.

2.3. *Numerical Procedure*

Assuming steady state, the ionization equilibrium is given by the solution of

$$\frac{x_j(i+1)}{x_j(i)} = \frac{\int_{\nu_{i,j}}^\infty (4\pi J_\nu/h\nu)\alpha_{1,j}^\nu(i)d\nu}{n_e \sum_{n=1}^\infty \alpha_{n,j}^i(T_e)} \quad (5)$$

for the ionization fraction x of species j in the ith stage of ionization; $a_{1,j}^\nu$ is the ground-state photoionization cross section for the species (j, i), and the α_n are the recombination coefficients. (The assumption of ionization equilibrium is reasonable even though the low densities of interest here imply that the recombination time scale $\tau_{\rm rec}$ may be quite long, since the ionization time is much shorter than the dynamical time scale. Solution of the time-dependent ionization equation shows that equilibrium is reached on a time scale $\tau_{\rm equil} \approx \tau_{\rm ion}$ when $\tau_{\rm ion} \ll \tau_{\rm rec}$.) Because of the geometry, the on-the-spot approximation is not always accurate: photons produced by ground-state recombinations may escape out of the disk to infinity. The mean intensity on the right-hand-side of equation (5) depends on the ionization state due to the diffuse source terms. An iterative scheme (Williams 1967) is used to solve the equations. Since the system is symmetric about the midplane of the disk, only one-half of the equilibrium needs to be calculated. The gas layer is divided into 25 zones. Starting at the outer boundary of the gas layer, an initial estimate of the ionization is obtained using the on-the-spot approximation and

ignoring the diffuse terms. This initial estimate is used to calculate the diffuse ionization terms, which are then included in the total ionization rate and the ionization equilibrium recalculated. This process is repeated until convergence is obtained; reaching an accuracy of 10^{-3} in the ionization fractions of H and He never requires more than a few iterations.

The ionization equilibrium is a function of the gas temperature. Rather than calculating the thermal balance, however, I have assumed that the gas temperature is 10^4 K at all radii and Z-heights. This is not solely for computational simplicity, but also because the temperature will depend on the metallicity and density (including the effects of clumping as well as the large-scale equilibrium) of the gas at these large galactocentric distances, which is unknown. (The temperature also enters into the vertical density calculation, assuming that the gas velocity dispersion is largely thermal at large radii.) In fact, unless the gas is quite clumped into discrete clouds, temperatures of order 10^4 K are expected for the range of ionization parameters present here, with little dependence on metallicity. The ionization parameter, $U = n_\gamma/n_{\rm H}$ (where n_γ is the ionizing photon number density and $n_{\rm H}$ is the atomic hydrogen number density), for the unattenuated ionizing photon field and one-sided irradiation is $U = 6.3 \times 10^{-4}\ I_{\rm Ly}/\alpha n_{-3}$, where n_{-3} is the hydrogen number density $n_{\rm H}/10^{-3}$. The typical number densities in the models range between $\sim 10^{-2}$–10^{-4} cm^{-3}, depending on (R, Z) and the particular galaxy model (see § 3). The calculations of Donahue & Shull (1991) (cf. their eqs. [5] and [6]) suggest temperatures of 10,000–20,000 K for these ionization parameters, for metallicities $\lesssim 0.1$ times solar. If the gas is somewhat clumpy, the clump temperatures can be lower, but will presumably still be several thousand K unless the ISM is cloudy with a very high cloud/intercloud density contrast: even for densities as high as $n_{\rm H} \sim 1$ cm^{-3}, so that $U \sim 5 \times 10^{-7}$, the gas temperature remains at $T \sim 8000$ K whether it is mostly ionized or neutral. Presumably only self-gravitating clouds can attain high enough densities to cool to low (~ 100 K) temperatures, since the low ISM pressures at these large galactocentric radii will preclude the existence of cold clouds as a pressure-equilibrium phase. The paucity of 21 cm absorption in the outer Milky Way also suggests that the atomic gas outside the optical disks of galaxies will be largely in a warm, low-density phase.

The error introduced by the assumption of a single temperature in the calculation of the ionization equilibrium is therefore probably minor compared to the uncertainties in the physical state of the gas. Since there will be a temperature gradient with both radius and height above the midplane, this assumption underestimates the ionization at large R and Z, leading to an underestimate of the critical column density at which the gas becomes largely ionized.

3. VERTICAL DISTRIBUTION OF GAS IN A DISK GALAXY

Since the ionization structure of the gas depends on the local gas densities, it is necessary to determine the equilibrium gas vertical distribution for a given column density. The mass surface density in atomic hydrogen at the large radii of interest here is generally negligible in comparison to the total surface density of dark matter necessary to explain the flatness of rotation curves, although it will greatly exceed the surface density of any constant mass-to-light ratio exponential disk. Hence the dark matter halo will dominate the potential. If the gas is in equilibrium, the vertical density distribution of the gas will be determined by its response to the halo potential.

The gas Z-distribution will depend on the surface densities of the disk, halo, and gas components, the density distribution in the halo, and the velocity dispersion(s) characterizing the gas Z-velocities. This problem is examined in more detail in Maloney (1993), which discusses the constraints that can be placed on the flattening of halos from observations of the thickness of neutral hydrogen layers in galaxies. For simplicity, I assume that the gas has an isothermal velocity distribution. This is in general agreement with the observational data on the Z-velocity dispersions in galaxies. Studies of nearly face-on galaxies have shown that the vertical velocity dispersions are typically in the range $\sigma_{zz} \approx 6$–10 km s^{-1}, with little or no radial variation (van der Kruit & Shostak 1982; Shostak & van der Kruit 1984; Dickey, Hanson, & Helou 1990). Although components with much higher velocity dispersions are present in the solar neighborhood (Kulkarni & Fich 1985; Lockman & Gehman 1991), they represent a relatively small fraction of the total hydrogen surface density ($\sim 20\%$–30%). Furthermore, the existence of these high-velocity components is presumably related to the rate of energy injection into the ISM by stars through stellar winds, supernovae, etc.; at the radii of interest for this problem, far outside the optical disk, the energy input from these processes will be negligible. A velocity dispersion of a few km s^{-1} is also comparable to the thermal speed of gas at several thousand K; the constancy of the measured value of the velocity dispersion across galactic disks, in which the atomic ISM probably undergoes a transition from cool cloud-dominated (where σ_{zz} measures the cloud-cloud velocity dispersion) to a more smoothly distributed warm neutral medium (where σ_{zz} presumably reflects the gas kinetic temperature) is rather intriguing.

With the assumption of isothermality for gas, the determination of $n_{\rm H}(Z)$ is simplified to calculating the response of an isothermal fluid to the halo potential. Since the halo dominates the potential at large radii, it determines both the circular velocity $V_c(R)$ and the vertical acceleration K_z. I have assumed axisymmetry and that the galaxy consists solely of a disk and a dark halo.

Calculation of the vertical density distribution of the gas requires the solution of two equations: Poisson's equation and the first moment of the Boltzmann equation in the Z-direction. In an axisymmetric system, Poisson's equation can be approximately integrated as

$$K_z = 2\pi G\Sigma(R, Z) + \frac{1}{R}\left[\frac{\partial}{\partial R}(RK_R)\right]Z ,$$

$$= 2\pi G\Sigma(R, Z) - \frac{1}{R}\left\{\frac{\partial[V_c^2(R)]}{\partial R}\right\}Z , \qquad (6)$$

provided that $\partial(RK_R)/\partial R$ doesn't vary very rapidly with Z (see Kuijken & Gilmore 1989); $\Sigma(R, Z)$ is the surface density in the disk between $\pm Z$ and $V_c(R)$ is the circular velocity at radius R. For a flat rotation curve, the second term on the right-hand-side of equation (6) is zero, so that equation (6) reduces to

$$K_z = 2\pi G\Sigma(R, Z) \qquad (7)$$

and the problem becomes one-dimensional. Comparison of equation (7) with the exact vertical forces in models of NGC 3198 shows that the approximate K_z values are in error by no more than 10% at all radii and Z-heights of interest.

From the assumption of isothermality, the first moment of the Boltzmann equation in Z is

$$\sigma_{zz}^2 \frac{\partial \rho_g(Z)}{\partial Z} = -\rho_g(Z) K_z , \quad (8)$$

where $\rho_g(Z)$ is the gas density at height Z. Since this is simply the equation of hydrostatic equilibrium, it does not matter whether the gas is in clouds or smoothly distributed: for a given velocity dispersion the average volume density of gas will be the same. In fact, as discussed above, there is some evidence that the atomic gas at large radii in galaxies is not in (cold) clouds. Photoionization models will also fail to produce the observed sharp edge to the neutral hydrogen in NGC 3198 if the gas is in relatively dense clouds; see the discussion in § 6.

The coupled equations (7) and (8) are solved numerically for a given galaxy model and gas column density. The galactic potential is assumed to consist of an exponential disk and a spheroidal halo; the disk is chosen to have a sech^2 (Z/Z_0) vertical density profile with a scale height equal to one-fifth the disk radial scale length (e.g., van der Kruit 1988), but the actual vertical density distribution in the disk has little influence on the gas density profile. The mass-to-light ratio of the disk is a free parameter in the models, but it introduces minimal uncertainty: at the large radius where the H I disk is truncated in NCG 3198, the atomic hydrogen dominates the (visible) disk surface density, and the halo density at large radii is not significantly changed by altering the disk parameters. The gas self-gravity is specifically included, as it has a nonnegligible effect on the density distribution. I have assumed that the halo and (stellar) disk potentials are fixed and do not respond to the gas. For the disk this becomes a poor assumption at large radii, but the stellar disk surface density is negligible here anyway.

The halos in these models are assumed to have oblate spheroidal density profiles, i.e.,

$$\rho(m^2) = \rho_c \left(1 + \frac{m^2}{r_c^2}\right)^{-1} \quad (9)$$

where

$$m^2 = R^2 + \frac{Z^2}{1 - e^2} \quad (10)$$

(cf. Binney & Tremaine 1987); here ρ_c and r_c are the halo central density and core radius and e is the halo eccentricity. This form is chosen solely because it produces asymptotically flat rotation curves with the asymptotic velocity

$$V_A^2 = 4\pi G \rho_c r_c^2 (1 - e^2)^{1/2} \frac{\arcsin(e)}{e} . \quad (11)$$

For $e = 0$ equations (9) and (11) reduce to the nonsingular isothermal sphere.

Current observations do not generally place very good constraints on the halo parameters individually (Lake & Feinswog 1989). In addition, the shapes of halos are not well determined, although there is evidence from the study of polar-ring galaxies that they are not extremely flattened (Whitmore, McElroy, & Schweizer 1987; Sackett & Sparke 1990) and observations of the flaring of neutral hydrogen layers in edge-on galaxies can rule out very flattened (axial ratio $q \sim 0.1$) halos (Maloney 1993). As will be seen in § 5, however, the results of the ionization calculations are not very sensitive to the halo eccentricity or to the precise values of the halo parameters. This is because the equipotential surfaces are always rounder (by about a factor of 3) than the equidensity surfaces; thus reducing the halo axial ratio from 1 ($e = 0$) to 0.1 ($e = 0.995$) only increases the midplane densities by a factor of $\simeq 3$.

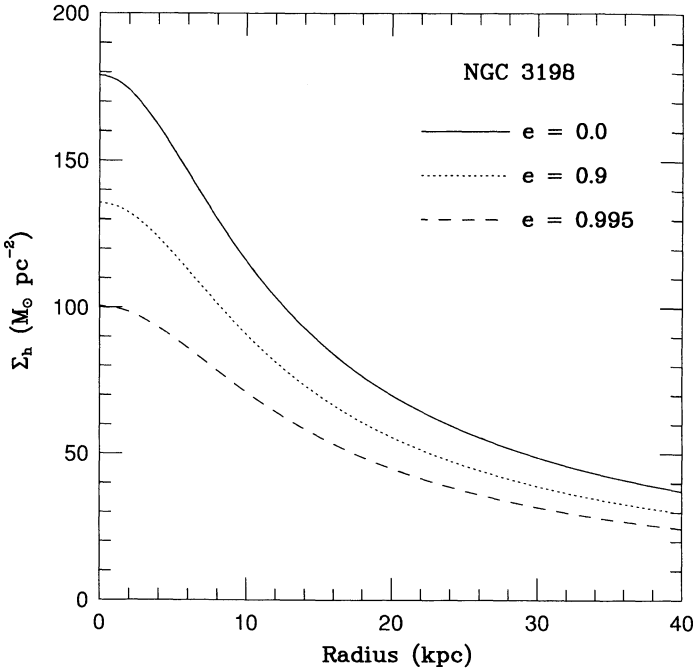

FIG. 1.—Halo surface densities for three models of NGC 3198 with eccentricities $e = 0$, 0.9, and 0.995, corresponding to axial ratios $q = 1.0$, 0.44, and 0.1, respectively. The halo core density and core radius parameters are $(\rho_c, r_c) = (6.7 \times 10^{-3}, 8.5)$, $(1.10 \times 10^{-2}, 9.0)$, and $(3.2 \times 10^{-2}, 10.0)$ ($M_\odot$ pc^{-3}, kpc) for the $e = 0$, 0.9, and 0.995 models.

Figure 1 shows the halo surface densities Σ_h as a function of radius for three models of NGC 3198, with halo eccentricities of 0, 0.9, and 0.995, corresponding to axial ratios of 1.0, 0.44, and 0.1. These models produce essentially identical rotation curves. (The halo central densities ρ_c and core radii r_c have been adjusted to match the observed rotation curve to within the errors; see the caption to Fig. 1.) In Figure 2 typical vertical density profiles $n_H(Z)$ for the gas as a function of radius in the three models are shown, assuming a constant ratio of gas to halo surface densities and a constant gas velocity dispersion of 9 km s^{-1}. Observations of neutral hydrogen at large radii in galaxies show that the ratio of gas surface density to halo surface density tends to change only slowly with radius (Bosma 1981; Carignan & Beaulieu 1989; Carignan et al. 1990). At a given radius, the midplane densities increase and the thickness of the gas layer drops as the eccentricity increases. For the remainder of this paper I generally use $\sigma_{zz} = 6$ or 9 km s^{-1}, which approximately bracket the observed range of neutral gas velocity dispersions.

4. ANALYTIC ESTIMATE AND SCALING RELATIONS

Before proceeding to the numerical calculations, it is worthwhile making a more careful analytic estimate of the critical column density discussed in § 1. This not only helps underscore the important physics involved but also provides scaling relations for the variation of N_c with the model parameters.

Consider a gas disk in equilibrium in a galactic potential, well outside the optical disk so that the only source of ionizing

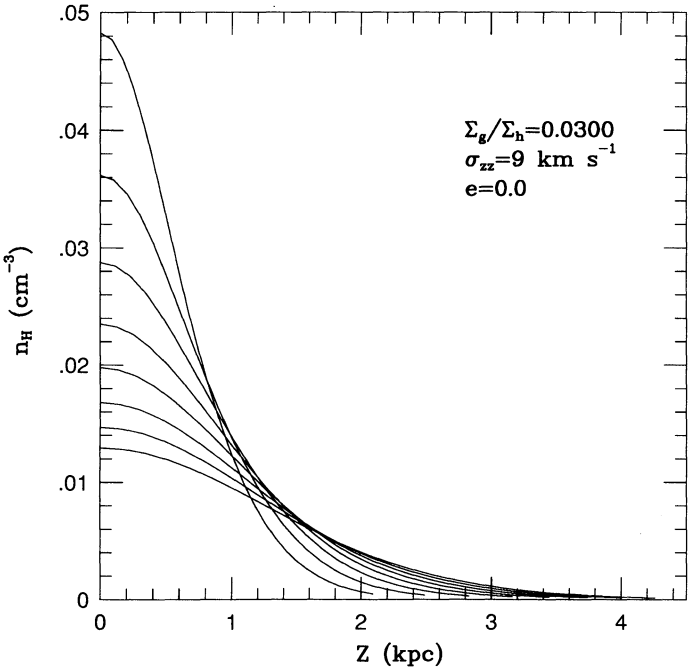

FIG. 2a

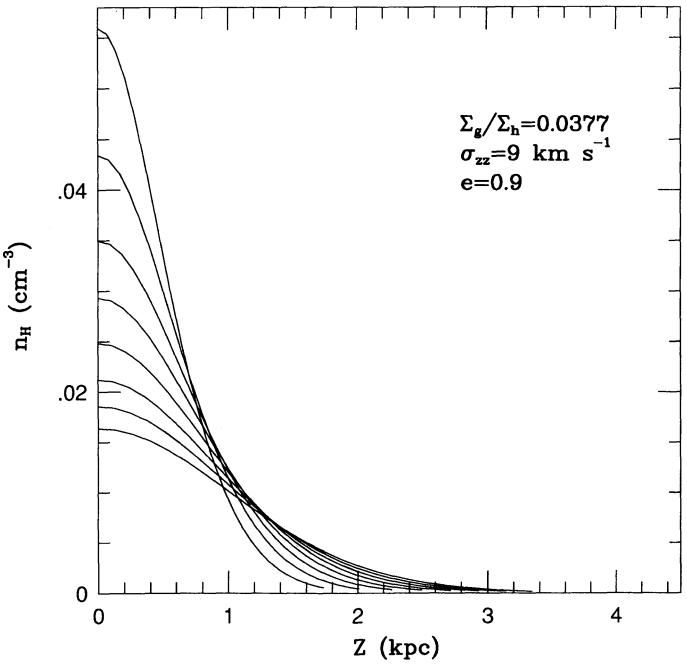

FIG. 2b

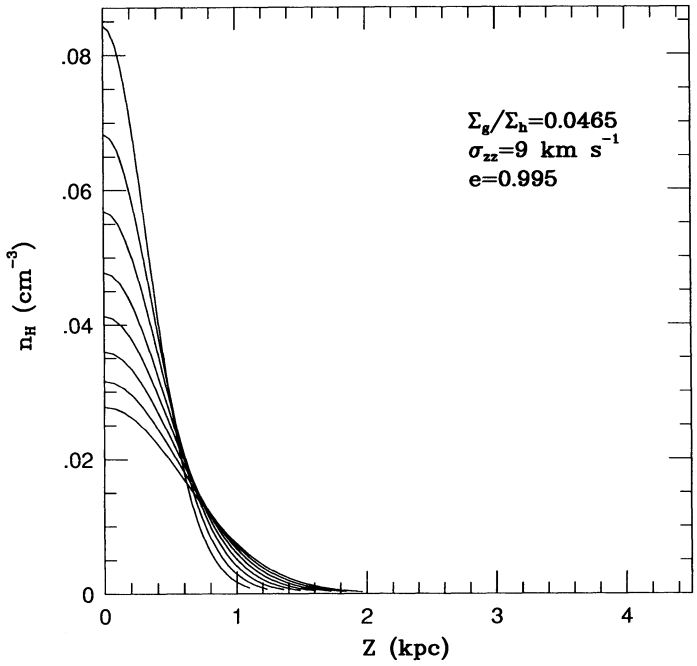

FIG. 2c

FIG. 2.—Typical halo density profiles for the three NGC 3198 models. The halo number densities as a function of height Z above the plane are plotted for R = 16, 18, 20 ... 30 kpc for (*a*) e = 0.0, (*b*) e = 0.9, and (*c*) e = 0.995. The ratio of gas to halo surface densities is assumed constant; this ratio is larger for the eccentric halo models in proportion to their lower surface densities, i.e., the gas surface density is assumed to be the same in all three models.

photons is the extragalactic background. If we ignore the change in the halo density with height Z above the midplane (which is a good assumption except for very flattened halos), then in the limit of negligible self-gravity the gas vertical distribution will be a Gaussian,

$$n_H(Z) = n_H(0)e^{-Z^2/2\sigma_h^2} \tag{12}$$

where the dispersion

$$\sigma_h = \frac{(r_c^2 + R^2)^{1/2}}{(4\pi G\rho_c r_c^2)^{1/2}}\,\sigma_{zz}\,. \tag{13}$$

The midplane density is

$$n_H(0) = \frac{N_H^{tot}}{(2\pi)^{1/2}\sigma_h}\ \mathrm{cm}^{-3} \tag{14}$$

and so also

$$N_H^{tot} = (2\pi)^{1/2}\sigma_h\, n_H(0)\,. \tag{15}$$

Assume there is a flux $\phi_{i,ex}$ photons cm^{-2} s^{-1} of ionizing photons normally incident on the top of the gas disk. This photon flux will ionize the gas approximately to the depth at which the column recombination rate equals the ionizing photon flux, i.e.,

$$\int_Z^\infty \alpha_{rec}\, n_e^2(Z')dZ' = \phi_{i,ex} \tag{16}$$

assuming $n_{H^+} = n_e$. Then the equivalent critical column density to the constant-density case discussed in § 1, at which the total column recombination rate just equals the ionizing photon flux, is implicitly given by equation (16) with $Z = 0$. Using equation (12) and integrating gives the result

$$\frac{\sqrt{\pi}}{2}\,\alpha_{rec}\, n_H^2(0)\sigma_h = \phi_{i,ex}\,.$$

Thus there is a critical midplane density

$$n_c = \left(\frac{2\phi_{i,ex}}{\sqrt{\pi}\alpha_{rec}\,\sigma_h}\right)^{1/2} \tag{17}$$

at which, for a given scale height σ_h, the gas will become completely ionized. Using equation (15), we can also express this criterion in terms of the critical column density,

$$N_c = \frac{2\sqrt{2}\phi_{i,\mathrm{ex}}}{\alpha_{\mathrm{rec}} n_{\mathrm{H}}(0)} \tag{18}$$

at which the gas column goes ionized for fixed midplane density $n_{\mathrm{H}}(0)$. Combining equations (17) and (18), the critical column density can be written

$$N_c = 2\pi^{1/4}\left(\frac{\phi_{i,\mathrm{ex}}\sigma_h}{\alpha_{\mathrm{rec}}}\right)^{1/2}. \tag{19}$$

Equation (19) can be put in a more useful form by noting that, for a spherical halo, the halo surface density integrated to infinity, $\Sigma_h(R) \equiv \int_{-\infty}^{\infty} \rho(R, Z)dZ$, is just

$$\Sigma_h(R) = \frac{\pi\rho_c r_c^2}{(r_c^2 + R^2)^{1/2}} \tag{20}$$

so that, using equation (11) with $e = 0$, the gas scale height can be written

$$\sigma_h = \frac{\sigma_{zz} V_{\mathrm{A}}}{4G\Sigma_h(R)}. \tag{21}$$

(For flattened halos there will be an additional numerical factor of order unity multiplying the right-hand-side of eq. [21], the precise value depending on the eccentricity.) Substituting this into equation (19) gives the critical column density as

$$N_c = \pi^{1/4}\left[\frac{\phi_{i,\mathrm{ex}}\sigma_{zz}V_{\mathrm{A}}}{\alpha_{\mathrm{rec}} G\Sigma_h(R)}\right]^{1/2}$$

$$= 1.7 \times 10^{19}\left[\frac{\phi_{i,4}\sigma_{zz,6}V_{\mathrm{A},100}}{\Sigma_{h,100}(R)}\right]^{1/2} \mathrm{cm}^{-2} \tag{22}$$

where $\phi_{i,4} = \phi_{i,\mathrm{ex}}/10^4$ photons cm^{-2} s^{-1}, $\sigma_{zz,6} = \sigma_{zz}/6$ km s^{-1}, $V_{\mathrm{A},100} = V_{\mathrm{A}}/100$ km s^{-1}, and $\Sigma_{h,100} = \Sigma_h/100\ M_\odot$ pc^{-2}, and I have used α_B at $T_e = 10^4$ K for α_{rec}. Thus for fixed galaxy parameters, equation (22) predicts that $N_c \propto \phi_{i,\mathrm{ex}}^{1/2}$, while for fixed $\phi_{i,\mathrm{ex}}$ and σ_{zz}, it predicts $N_c \propto [V_{\mathrm{A}}/\Sigma_h(R)]^{1/2}$. These scaling relations will be compared to the numerical results below.

5. RESULTS

In this section the photoionization models are used in conjunction with the gas density distributions to calculate the neutral gas fractions as a function of radius in galaxies, with particular application to NGC 3198. The models of §§ 2 and 3 are combined to model the neutral hydrogen distribution in NGC 3198 in the following manner: first a mass model for the galaxy is calculated to match the observed rotation curve; this will depend (weakly) on the choice of disk M/L and on the halo eccentricity. The disk is assumed to have a scale-length of 2.68 kpc, the value derived from surface photometry (van Albada et al. 1985). Next the total atomic hydrogen column density $N_{\mathrm{H}}^{\mathrm{tot}}(R)$ is specified and the equilibrium gas distribution is calculated for a chosen value of σ_{zz}. The photoionization model is then used to calculate the neutral hydrogen column density $N_{\mathrm{H\,I}}(R)$ as a function of σ_{zz} and I_{Ly}.

An obvious strategy is to determine what total column density distribution with radius (for a particular mass model, σ_{zz} and I_{Ly}) produces a neutral column density distribution which matches the observed distribution. The ratio of total to neutral column density will be an increasing function of radius: since both the halo and gas surface densities decrease at larger R, the ionization fractions increase with radius. Eventually the total column density can exceed the neutral column density by orders of magnitude. Before attempting to match the NGC 3198 results in detail, however, it is instructive to examine the general behavior of the neutral column density as a function of radius; in particular, the transition radius at which the gas goes from mostly neutral to mostly ionized.

5.1. *Transition Region Models*

Since the results are not very sensitive to the specific mass model chosen, I have calculated the results for this transition region for a single model of NGC 3198. The rotation curve for this model and the model parameters are shown in Figure 3. Since the observed neutral hydrogen distribution is described reasonably well by an exponential with a scale length of 3.3 = 8.84 kpc (van Albada et al. 1985) I have assumed that the total hydrogen distribution is also described by an exponential with this same scale length. The total hydrogen column density has been set to $N_{\mathrm{H}}^{\mathrm{tot}} = 1.2 \times 10^{20}$ cm^{-2} at 20 kpc which approximately matches the observed neutral column density for $\sigma_{zz} \approx$ a few km s^{-1}, $I_{\mathrm{Ly}} \approx 1$.

The neutral column densities have been calculated for $\sigma_{zz} =$ 6 and 9 km s^{-1} and for $I_{\mathrm{Ly}} = 1$, 2, 3, and 5. The total and neutral column densities are plotted as a function of radius in Figure 4. (The scaling between column density and radius is of course determined in this case solely by the choice of radial scale length of the atomic hydrogen distribution.) At $R = 20$ kpc the neutral fraction is $\gtrsim \frac{2}{3}$ for all of the models; the models are not plotted for smaller radii since the results are uninteresting. The behavior of $N_{\mathrm{H\,I}}$ as a function of radius is similar for all the values of σ_{zz} and I_{Ly}: the neutral fraction declines fairly slowly with radius until a critical column density (which is a function of σ_{zz} and I_{Ly}) is reached. At this column density the

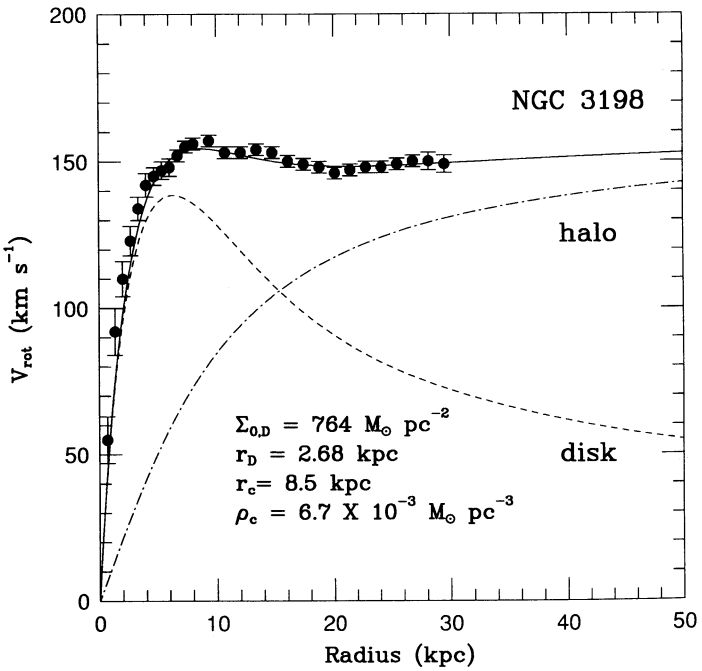

FIG. 3.—Rotation curves for the disk, halo, and sum for the $e = 0.0$ model of NGC 3198 used in the models.

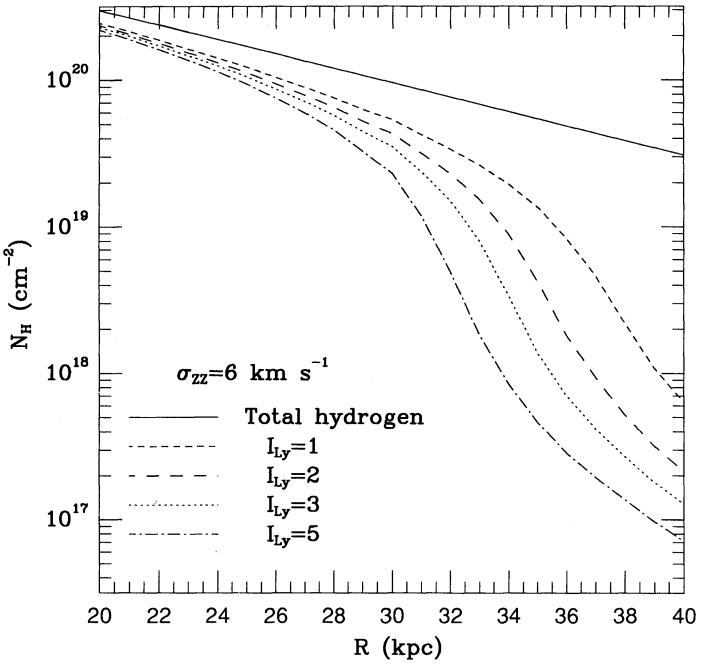

FIG. 4a

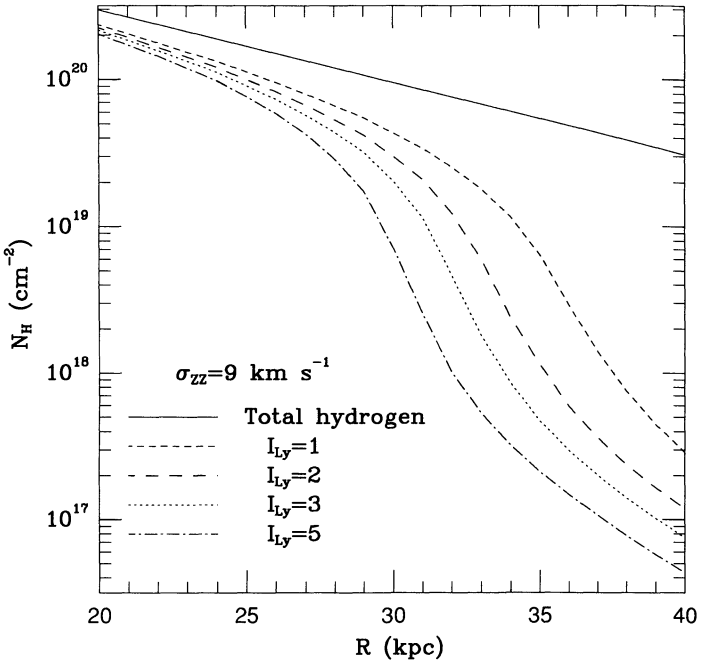

FIG. 4b

FIG. 4.—Total and neutral hydrogen column densities for the transition region models. The total hydrogen column density is assumed to vary exponentially with a radial scale length of 8.8 kpc, and is set to $N_H^{tot} = 1.2 \times 10^{20}$ cm^{-2} at $R = 28$ kpc. The neutral hydrogen column densities have been calculated for four different values of the radiation field scaling parameter $I_{Ly} = 1$, 2, 3, and 5, and for two different vertical velocity dispersions: (*a*) $\sigma_{zz} = 6$ km s^{-1} and (*b*) $\sigma_{zz} = 9$ km s^{-1}.

neutral fraction begins to decrease more rapidly, so that the neutral gas column density drops by more than an order of magnitude, within a radial increment $\Delta R \approx 3$–5 kpc: ΔR decreases with increasing I_{Ly}. For all these models this critical column density $N_c \sim$ a few times 10^{19} cm^{-2}.

Figure 5 plots the neutral hydrogen fraction X_H against Z-height for radii between 20 and 40 kpc; the Z-profiles have been normalized to the maximum Z-height, Z_{max}. Results are shown for two different models, with $I_{Ly} = 1$ and $I_{Ly} = 5$. Interior to the transition radius the gas is nearly neutral out to some fraction of Z_{max}; this produces the "step" visible in Figure 5. The maximum Z/Z_{max} for which the gas is nearly neutral declines with increasing radius; below the critical column density, the neutral fraction is always small and declines smoothly with increasing R and Z.

The rapid decrease in the neutral fraction with increasing R and Z means that the observable (neutral) hydrogen distribution will be very different from the total hydrogen distribution. This is shown graphically in Figure 6, which plots two-dimensional slices through the symmetry axis of the model gas distributions for the total and neutral hydrogen. (This would correspond to a $V = V_{max}$, V_{min} slice for a galaxy with a flat rotation curve.) The contour levels for the two distributions are the same. The neutral gas volume densities decline much more rapidly with both R and Z than do the total gas volume densities. Thus observations of the neutral component can give a very misleading picture of the total gas distribution in a galaxy. For example, Figure 7 shows the Z-height at which the gas density has fallen to half the midplane value, $Z_{1/2}$, as a function of radius, for the total and neutral hydrogen densities. Whereas $Z_{1/2}$ for the total gas density increases monotonically with R, the thickness of the neutral gas distribution peaks at $R = 27$ kpc and declines swiftly with increasing R. (The secondary increase beyond $R = 35$ kpc results from the disappearance of the neutral "step" near the midplane, as can be seen from Figure 5. The neutral gas densities are so small at this point, however, that this gas would be completely unobservable.)

5.2. *Detailed Models of NGC 3198*

Here I apply the photoionization models specifically to the observations of NGC 3198 and determine the total hydrogen column density (for a given σ_{zz}, I_{Ly}) which corresponds to the measured neutral hydrogen column density. The neutral hydrogen column density as a function of radius along the major axis was derived from the VLA observations and was kindly provided by Jacqueline van Gorkom. The neutral column densities have been corrected for inclination i using $i(R)$ from Begeman (1989). There are significant differences between the neutral hydrogen distributions along the NE and SW side of the galaxy. The neutral hydrogen drops below detectable levels more than 6 kpc further out from the center on the SW major axis. If the H I edge in NGC 3198 is simply a physical edge to the gas distribution, this fact indicates that it cannot be long-lived (van Gorkom 1991). Thus I have modeled the two sides of the major axis separately. As the results are insensitive to the exact mass model, most results have been calculated for the mass model shown in Figure 3.

Figure 8 plots the *observed* $N_{H\,I}(R)$, along with the *inferred* $N_H^{tot}(R)$ which matches the observed neutral hydrogen column densities, for the major axis cuts for $I_{Ly} = 6$ and 9 km s^{-1} and $I_{Ly} = 1$, 2, and 5. (The last point on the SW side is the 3 σ upper limit of 4×10^{18}; using the 1 σ value instead would lower the total column densities at that point by $\approx$20%.) The total column density inferred from the observed $N_{H\,I}$ varies with velocity dispersion and intensity of the radiation field, but

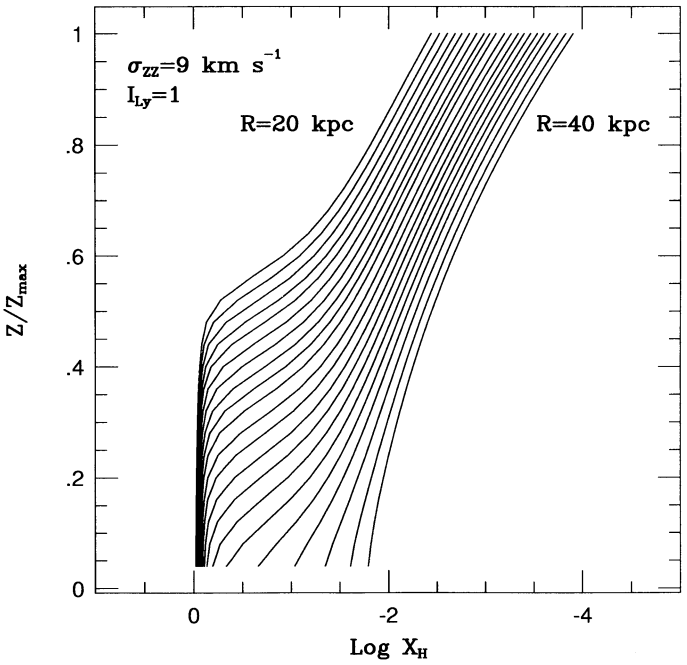

FIG. 5a

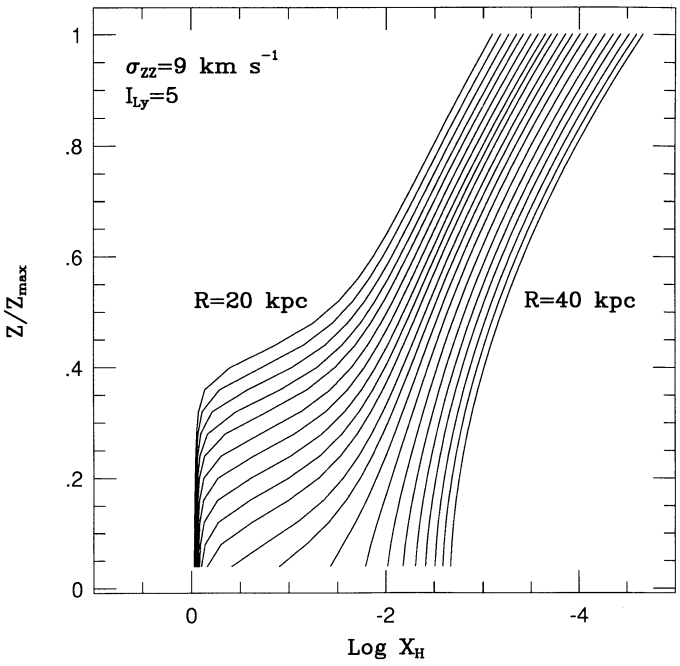

FIG. 5b

FIG. 5.—Neutral hydrogen fraction X_H as a function of height Z above the plane for the transition region models, for radii R = 20, 21, 22, ... 40 kpc. The values at each radius have been normalized to the maximum Z-height Z_{max} for ease of comparison. $X_H(R, Z)$ is plotted for σ_{zz} = 9 km s^{-1} for (*a*) I_{Ly} = 1 and (*b*) I_{Ly} = 5.

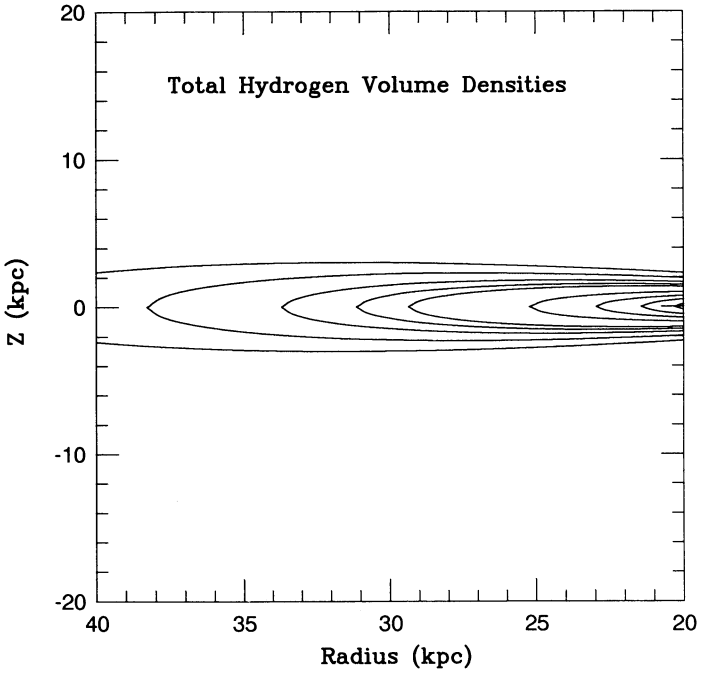

FIG. 6a

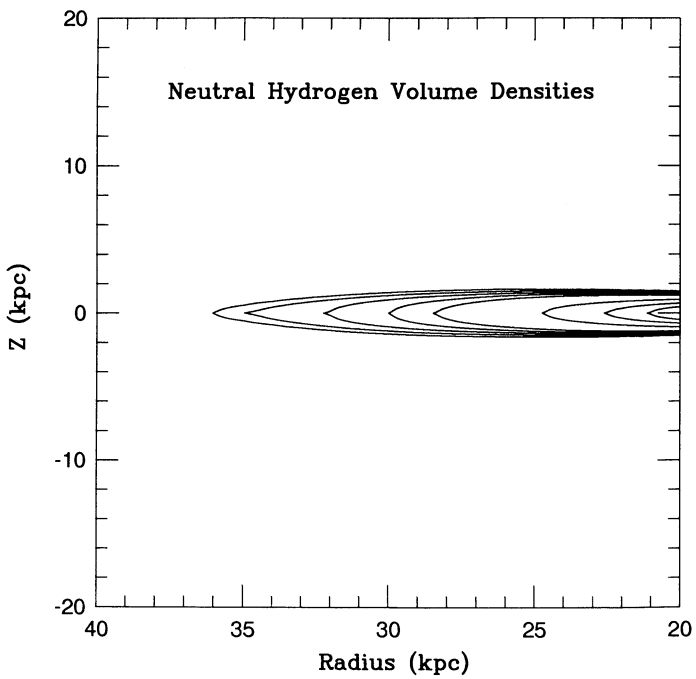

FIG. 6b

FIG. 6.—Contour plots of the total and neutral gas volume densities in an (R, Z) slice through the symmetry axis for the transition region models (for σ_{zz} = 9 km s^{-1}, I_{Ly} = 1). The contour levels are 7.5 × 10^{-3}, 5.0 × 10^{-3}, 2.5 × 10^{-3}, 1.0 × 10^{-3}, 0.01, 0.02, 0.03, 0.04, and 0.05 cm^{-3} in both plots. The total hydrogen volume densities are plotted in (*a*) and the neutral hydrogen volume densities in (*b*).

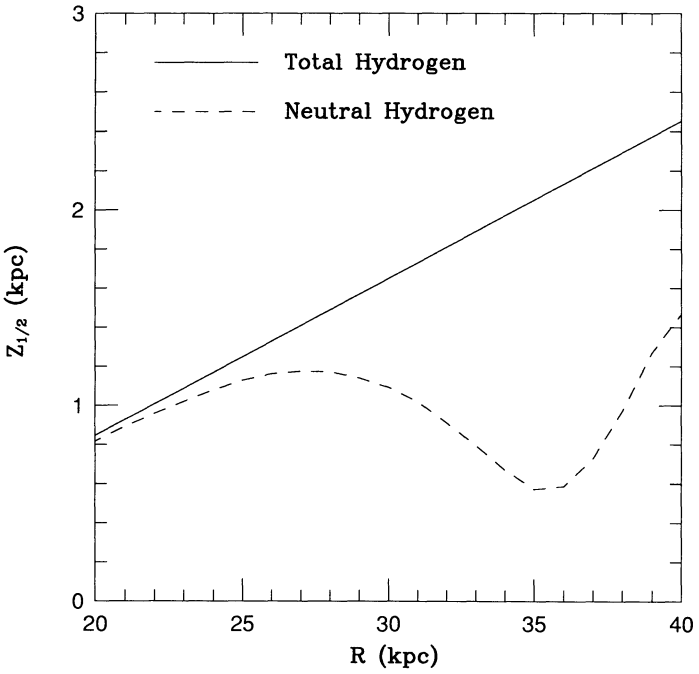

FIG. 7.—The height at which the gas volume density has dropped to half of the midplane density, $Z_{1/2}$, as a function of radius for the total and neutral hydrogen.

not strongly. At radii where the gas is largely ionized, N_H^{tot} varies as expected from the analytic results derived in § 4, i.e., as $\sigma_{zz}^{1/2}$ and $\phi_{i,ex}^{1/2}$. It is worth reiterating that the models will tend to underestimate the total column density as the ionized fraction becomes large, due to temperature variations and the breakdown of the plane-parallel approximation in calculating the attenuation of the ionizing photon flux. Also, as expected from § 3, the results are insensitive to the halo eccentricity; the maximum decrease in total column density for an $e = 0.995$ halo is only $\sim 30\%$ from the $e = 0$ case. Other changes in the mass models (e.g., varying disk mass) produce changes of a few percent or less.

Since the basic premise of these models is that it is a change in the ionization state for the gas, rather than a change in the total column density, which gives rise to the sharp neutral hydrogen cutoff in NGC 3198, it is obviously unsatisfactory to have to appeal to substantial features in the total hydrogen distribution or marked asymmetry between the NE and SW halves of the galaxy in order to match the observed neutral hydrogen distribution. At first glance, the models shown in Figure 8 would seem to imply that the total hydrogen distribution is rather asymmetric.

That this is not really the case is demonstrated in Figure 9, which plots the observed $N_{H\,I}$ and the derived N_H^{tot} (for $\sigma_{zz} = 9$, $I_{Ly} = 1$) for the two sides of the galaxy. The differences in the total hydrogen distributions for the NE and SW major axis cuts are everywhere less than a factor of 2. As the ionized gas fraction becomes substantial, small differences in the total column densities are magnified in the neutral column densities. Hence, the total gas distribution is quite symmetric. To emphasize this point, in Figure 10 I have plotted the total gas distributions for the major axis cuts for the entire galaxy. For $R < 16.8$ kpc I have approximated the total column density by the neutral, since the correction at these column densities is small ($\lesssim 20\%$). Also plotted on the figure is an exponential distribution with scale length 10.9 kpc; it has been normalized simply so that it matches the average N_H^{tot} for the two sides over most of the range in radius for which there is overlapping data. (The choice of an exponential is intended solely to be illustrative, but it is obviously a reasonable fit.) The deviations of the total gas distribution from this exponential are less than 40% for the two halves of the major axis. Hence the total gas distribution is far more axisymmetric than would be inferred from the total hydrogen. This is a strong argument for the photoionization model.

The ratio of the total gas mass to the neutral gas mass increases as σ_{zz} and/or I_{Ly} are increased. The gas mass (including helium) derived from the neutral hydrogen data for radii between 16 and 40 kpc is $\sim M_{H\,I} \approx 2.4 \times 10^9\ M_\odot$. For $\sigma_{zz} = 9$ km s^{-1} and $I_{Ly} = 1$, the total gas mass for this radius range is twice this, $M_H^{tot} \approx 4.8 \times 10^9\ M_\odot$, and the total atomic hydrogen mass for the galaxy is $\sim 50\%$ larger than derived from the neutral gas alone. The total gas mass beyond 16 kpc could be substantially larger, depending on how far the gas disk extends.

The results presented here show that the sharp cutoff seen in the neutral hydrogen distribution in NGC 3198 is explicable as the result of photoionization of neutral gas in a smoothly varying gas disk by the extragalactic radiation field. This has significant implications for H I studies of galaxies and for the intensity of the extragalactic ionizing photon flux; I discuss these in the following section.

6. DISCUSSION

6.1. *Sharp Edges in Other Galaxies*

In the models presented here, it is the isotropic extragalactic radiation field that produces the sharp edge to the neutral hydrogen distribution seen in NGC 3198, rather than some local source of ionizing photons associated with the galaxy (e.g., OB stars or high-latitude white dwarfs). Hence for an axisymmetric galaxy, the column density at which the cutoff occurs should be independent of azimuth, as is seen NGC 3198. Since all galaxies will be subject to essentially the same ionizing background radiation field, we would expect a sharp edge to the neutral gas distribution to be a generic feature of gaseous galactic disks.

A good benchmark column density for the purposes of this discussion is the total column density at which $N_{H\,I}/N_H^{tot} = 0.1$, which will be denoted N_{cr}. Typically, increasing the total column density by $\sim 25\%$ above N_{cr} causes the neutral fraction to increase by a factor of ~ 3, while decreasing the column density by the same amount lowers the neutral fraction by about the same factor. Hence the neutral hydrogen fraction changes very rapidly above and below N_{cr}.

The insensitivity of the results for NGC 3198 to the degree of halo flattening and to the precise mass model suggests that N_{cr} will not be a very strong function of the galaxy mass parameters. To quantify this statement, I have determined N_{cr} as a function of radius for three different galaxy mass models. The first is the spherical mass model for NGC 3198 used for the calculations of § 5. The second and third are essentially scaled-up and -down versions of this model, with asymptotic halo velocities of 271 and 68 km s^{-1}, respectively. (The relative sizes of the disk and halo scale lengths have been adjusted to produce rotation curves that are nearly flat over the range of radii for which N_{cr} has been calculated.) Since the actual size

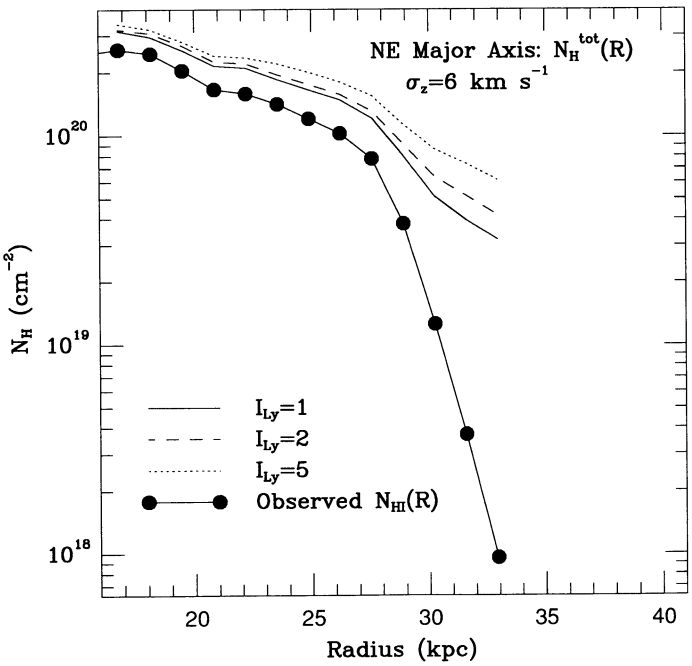

FIG. 8*a*

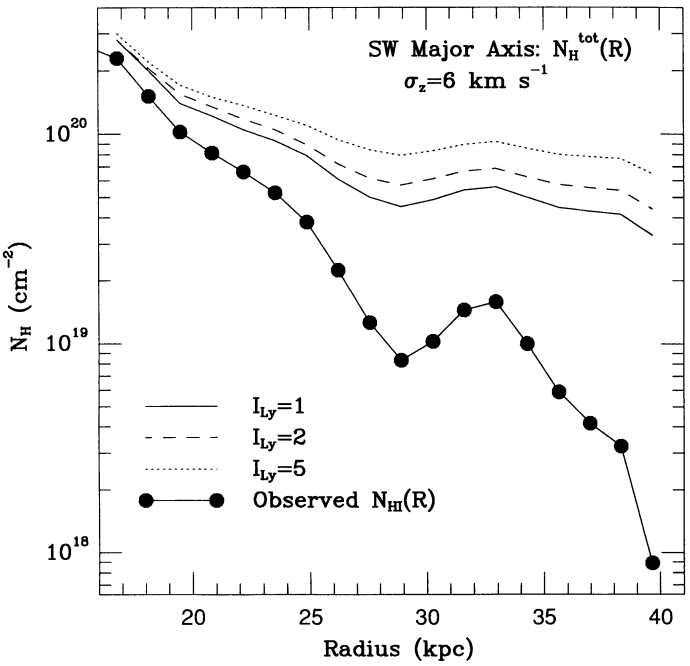

FIG. 8*b*

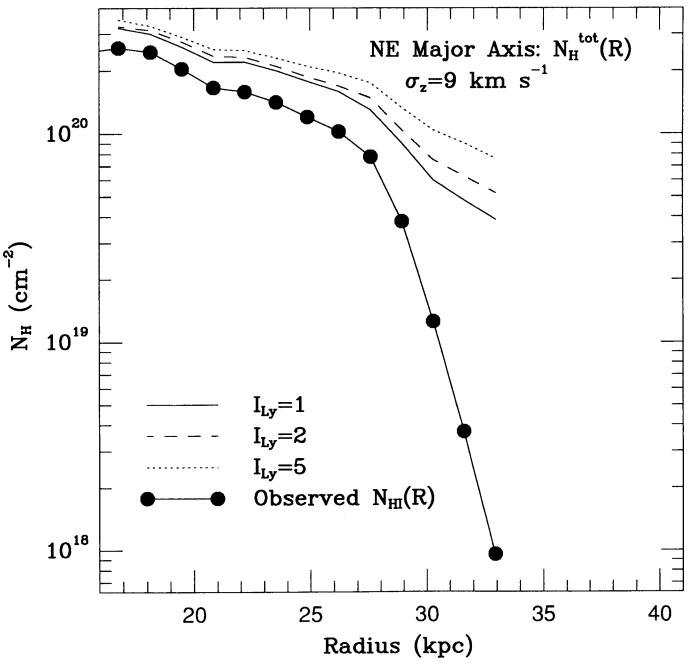

FIG. 8*c*

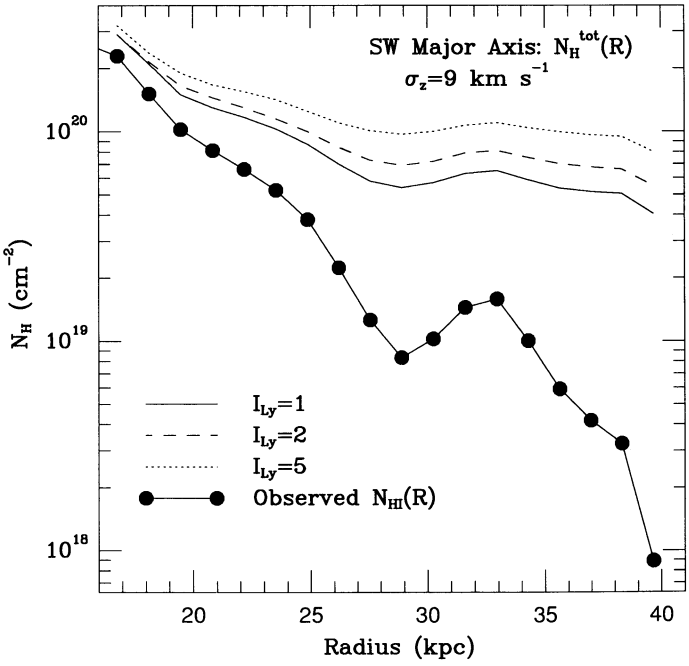

FIG. 8*d*

FIG. 8.—Total hydrogen column densities which match the observed neutral hydrogen column densities of van Gorkom et al. (1993) for different values of σ_{zz} and I_{Ly}. All of the models produce neutral hydrogen column densities which match the observed value to within 5%. The filled circles are the observed neutral hydrogen column densities, with an upper limit of $N_{HI} \lesssim 4 \times 10^{18}$ cm^{-2} assumed at 39.7 kpc. The derived total hydrogen column densities are plotted for the NE and SW major axis cuts for $I_{Ly} = 1, 2$ and 5 for (*a–b*) $\sigma_{zz} = 6$ km s^{-1} and (*c–d*) $\sigma_{zz} = 9$ km s^{-1}.

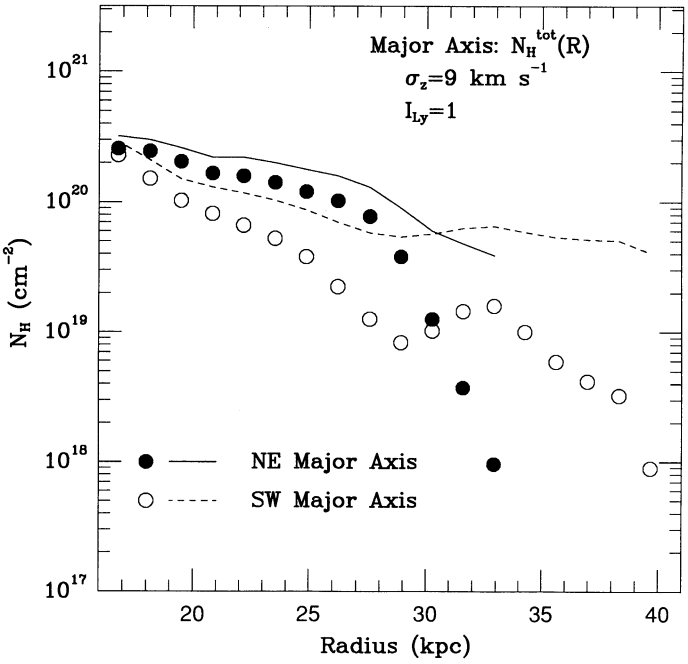

FIG. 9.—Observed $N_{H\,I}$ and derived N_H^{tot} for the NE (*filled circles, solid line*) and SW (*open circles, dotted line*) halves of the major axis, for $\sigma_{zz} = 9$ and $I_{Ly} = 1$.

scales are not of particular interest, I have instead used the halo surface density integrated to infinity (cf. eq. [20]) as the radial coordinate. For all radii at which N_{cr} was calculated, Σ_h dominates the total mass surface density by a substantial factor. The mass model parameters and the halo surface densities as a function of R are given in Figure 11.

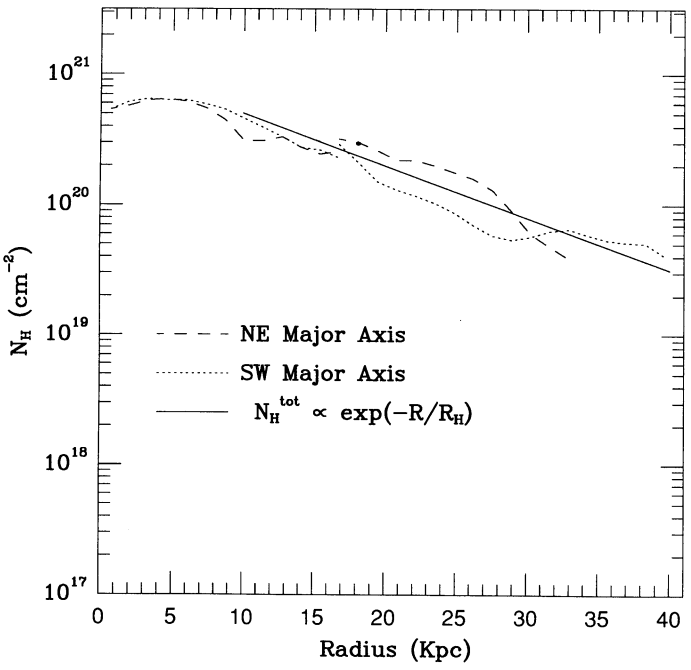

FIG. 10.—Approximate total hydrogen distribution for the major axis of NGC 3198. Derived N_H^{tot} values (for $\sigma_{zz} = 9$, $I_{Ly} = 1$) are plotted for $R > 16$ kpc; $N_{H\,I}$ from van Gorkom et al. (1993) is used at smaller radii. Approximate exponential fit has $R_H = 10.9$ kpc.

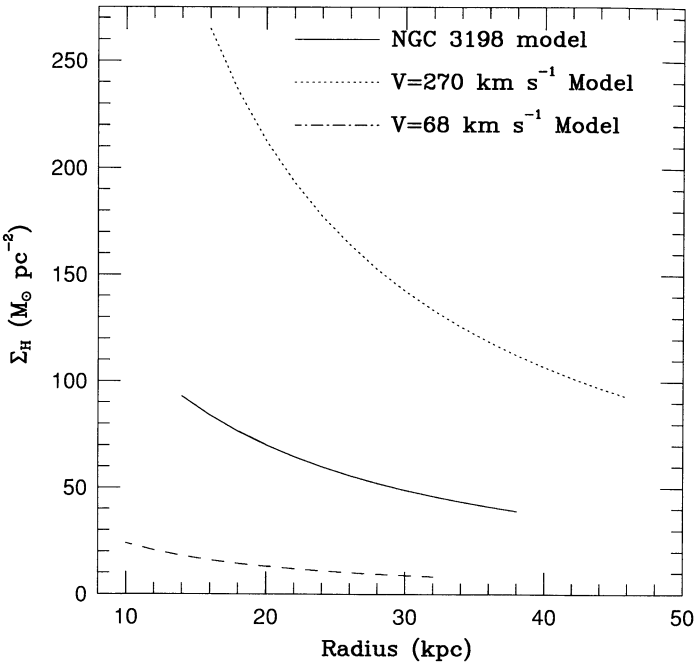

FIG. 11.—Halo surface densities as a function of radius for the three spherical mass models for which N_{cr} was calculated. The halo parameters are (ρ_c, r_c) = (6.7×10^{-3}, 8.5), (3.4×10^{-1}, 2.0), and (3.4×10^{-3}, 5.0). The first is the NGC 3198 model, with asymptotic halo velocity $V_A = 161$ km s^{-1}; the second and third have $V_A = 270$ km s^{-1} and $V_A = 68$ km s^{-1}, respectively. All three models have disk scale lengths $r_d = 2.68$ kpc; the central mass surface densities are $\Sigma_{0,d} = 764$, 1000, and 100 $M_\odot$ pc^{-2}, respectively. The rotation curves are nearly flat over the range of radii for which N_{cr} has been calculated; the halo surface densities are only plotted for that radius range for each model.

In Figure 12 I have plotted N_{cr} against Σ_h for two different velocity dispersions, $\sigma_{zz} = 6$ and 9 km s^{-1}, and two values of the ionizing photon flux, $I_{Ly} = 1$ and 5. The halo surface densities range from $\Sigma_h \simeq 8$ to 265 $M_\odot$ pc^{-2}. For fixed I_{Ly} and σ_{zz}, N_{cr} changes by less than a factor of 3 as the halo surface density changes by more than a factor of 30. For a given galaxy model N_{cr} changes by less than a factor of 2 with varying $\Sigma_h(R)$; the differences in N_{cr} between the different galaxy models for the same Σ_h are $\lesssim 50\%$. The calculated values of N_{cr} for the $\sigma_{zz} = 6$ and $\sigma_{zz} = 9$ km s^{-1} differ by 25%–30%, with a very weak dependence on halo surface density.

This is precisely the behavior expected from the analytic estimate of § 4. From equation (19), the critical column density depends on the density distribution only through $\sigma_h^{1/2}$, where σ_h is the gas scale height. In the absence of self-gravity, $\sigma_h \propto V_A/\Sigma_h(R)$; including the gas self-gravity will reduce the scale height, but at the column densities of interest here this effect will be moderate. Hence $N_{cr} \approx N_c \propto [\sigma_{zz} V_A/\Sigma_h(R)]^{1/2}$. The quantity $[V_A/\Sigma_h(R)]^{1/2}$ varies by less than a factor of 3 over all Σ_h for the three galaxy models, and by only a factor of 1.6–1.7 within a given model. The column density required to attenuate the ionizing flux sufficiently to allow a neutral "core" to survive at low Z thus does not depend strongly on the density distribution. This is why neglect of the gas self-gravity, as was done by Bochkarev & Sunyaev (1977), does not lead to large errors in the calculation of the neutral column densities, even though the local gas volume densities may be too low at the midplane by factors of ~ 3–4.

The analytic value for N_c is generally within 15% of the numerical value of N_{cr}. Since the neutral fraction is dropping

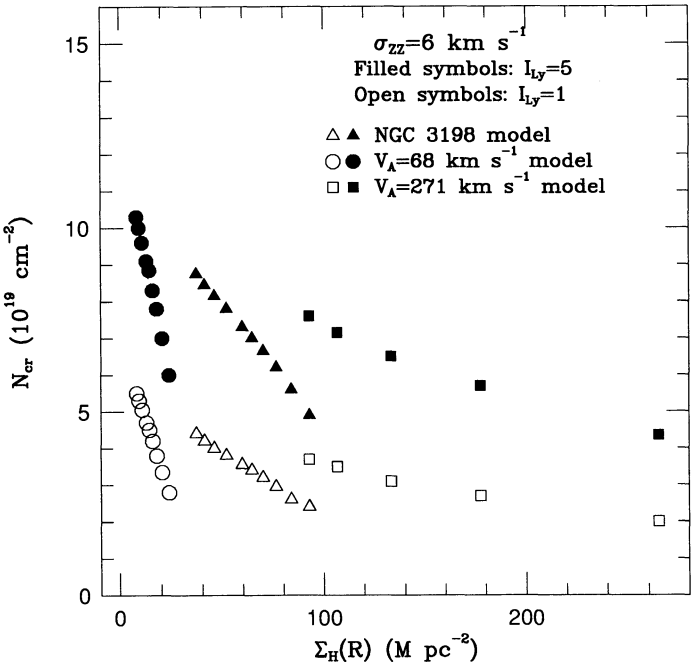

FIG. 12*a*

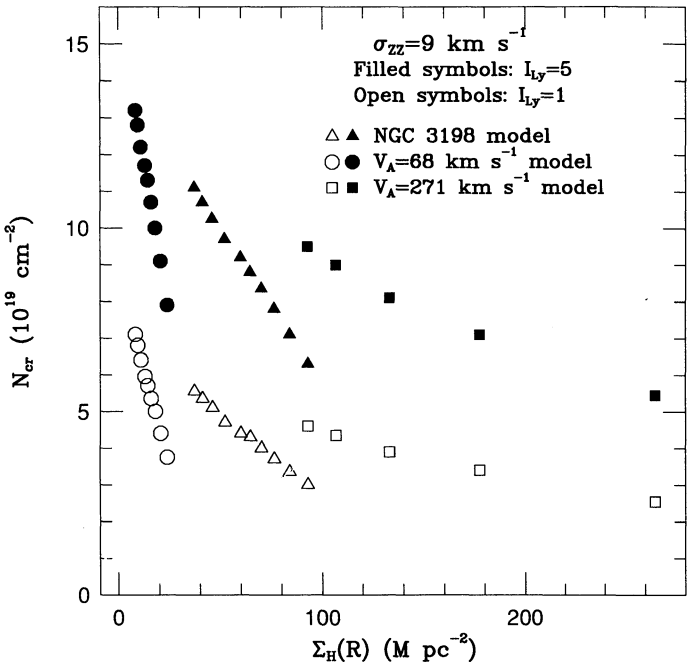

FIG. 12*b*

FIG. 12.—The critical column density $N_{cr} \equiv$ the total column density N_H^{tot} at which $N_{HI}/N_H^{tot} = 0.1$. N_{cr} has been calculated as a function of radius for the three different galactic models plotted in Fig. 10. The halo surface density integrated to infinity, $\Sigma_h(R)$, has been used as the radial coordinate. N_{cr} has been calculated for $I_{Ly} = 1$ and 5 for all three models, for (*a*) $\sigma_{zz} = 6$ km s^{-1} and (*b*) $\sigma_{zz} = 9$ km s^{-1}.

rapidly for column densities below N_{cr}, the precise value of N_{HI}/N_H^{tot} used to define N_{cr} is not crucial. As expected, N_{cr} is not very sensitive to the halo shape. Figure 13 shows N_{cr} for the NGC 3198 model for three halo eccentricities ($e = 0.0$, 0.9 and 0.995). The values of N_{cr} are only 30%–35% lower in the flat ($e = 0.995$) halo model than in the spherical halo model.

These results show that ionization by the extragalactic radiation field should produce a sharp cutoff to the observable neutral hydrogen column density in galaxies, *at a critical column density* $N_H^{tot} \approx N_{cr}$, *which is nearly independent of galaxy mass or size*. For a fixed value of σ_{zz} and I_{Ly}, N_{cr} varies by only a factor of $\sim$1.7 about the mean value. Hence a sample of galaxies observed to some column density limit below the typical value of N_{cr} (e.g., $N_{HI} \lesssim 5 \times 10^{18}$ cm^{-2}) will all show sharp neutral hydrogen edges, with very similar values of the truncation column density. (Of course, this requires a sample of galaxies whose gas distributions have not been disturbed by some other process, such as galaxy-galaxy interactions or an intracluster medium).

No such survey of galaxies with extended neutral hydrogen disks to low column densities of N_{HI} exists in the literature. However, using the Arecibo 305 m dish, Briggs et al. (1980) showed that neutral hydrogen column densities $N_{HI} \gtrsim 3 \times 10^{18}$ cm^{-2} at radii of 2–3 R_{Ho} are not common around spiral galaxies. In addition, a cutoff has probably been seen in the nearby dwarf Sc spiral M33. Corbelli, Schneider, & Salpeter (1989), using the Arecibo 305 m telescope, examined the radial behavior of the neutral hydrogen column density in a strip along the major axis in M33. They found that the neutral column density declined over a distance of 8 kpc from $N_{HI} \approx 2 \times 10^{20}$ to 3×10^{19}, corresponding to an *e*-folding length of $\sim$3.5 kpc, and then dropped precipitously by another order of magnitude in $\sim$1 kpc. This is very similar to what is seen in NGC 3198 and in agreement with the model predictions presented here.

There may also be more local evidence for this process. Cohen (1982) in a 21 cm study of high-velocity clouds in Cetus, mapped a large ($\sim$12°) complex centered near $l = 165°$,

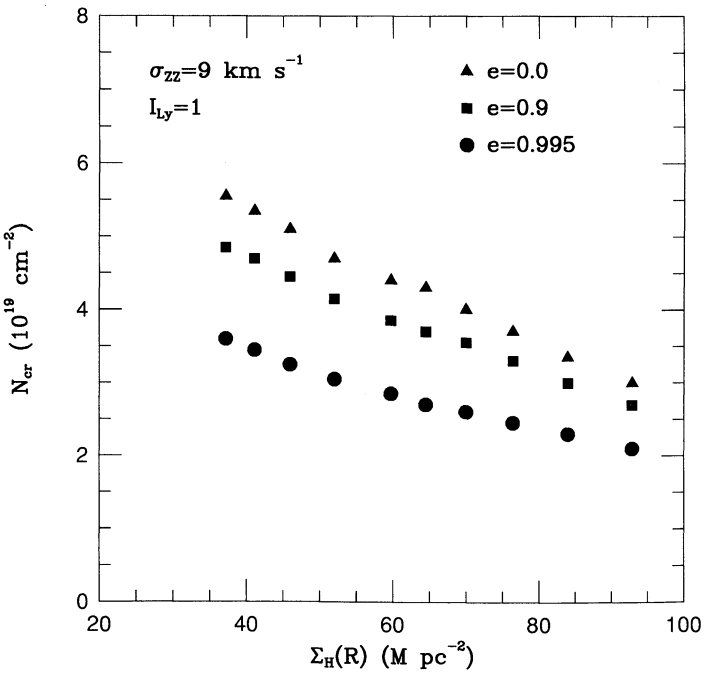

FIG. 13.—As in Fig. 11, but for the NGC 3198 models with eccentricities $e = 0.0$, 0.9, and 0.995, for $I_{Ly} = 1$ and $\sigma_{zz} = 9$ km s^{-1}.

$b = -45°$. Of relevance here is the fact that portions of the atomic gas complex have very sharp edges (at a minimum column density level of $N_{\rm H\,I} = 10^{19}$ cm^{-2}). Cohen suggested that this might be the result of pressure confinement by a hot Galactic halo. However, given the probable substantial Z-height of the high-velocity clouds, it is quite possible that these sharp edges are also the result of photoionization by the extragalactic background. The ionization equilibrium time scale for these clouds is shorter than the dynamical time scale (the clouds will travel $\sim$2.5 kpc in 10^7 yr: Cohen 1982). A possible detection of Hα emission from this complex was made by Kutyrev & Reynolds (1989). Confirmation of this result would be very informative.

6.2. *The Extragalactic Ionizing Flux*

Due to absorption by neutral gas in the disk of our own Galaxy, the extragalactic radiation field is unobservable at energies below a few hundred electron volts. The sharp edges which are produced in neutral hydrogen disks by this radiation field, however, make it possible to obtain an indirect estimate of the ionizing photon flux, as originally suggested by Sunyaev (1969). For the column densities of relevance here, only photons with energies between the Lyman limit and $E \sim 200$ eV contribute to the ionization. For fixed σ_{zz}, the model values of $N_{\rm cr}$ scales nearly as $\phi_{i,\rm ex}^{1/2}$, with almost no dependence on galaxy model, in agreement with the estimate in § 4. The model results presented here show that values of $\phi_{i,\rm ex} \gtrsim 10^4$ photons cm^{-2} s^{-1} provide a reasonable fit to the NGC 3198 results for smoothly varying, nearly axisymmetric gas distributions. If $\phi_{i,\rm ex}$ is much less than 10^4 photons cm^{-2} s^{-1}, $N_{\rm H}^{\rm tot}(R)$ must have substantial asymmetry and structure near the edge, which would make the photoionization models less appealing. However, $\phi_{i,\rm ex}$ also cannot be too large, or else the cutoffs would occur at a higher column density than observed; this is true for any total gas distribution which monotonically decreases with radius. In practice, the observational upper limit to $\phi_{i,\rm ex}$ is probably lower than the value where this latter constraint would become significant, but $\phi_{i,\rm ex}$ could not be much larger than the maximum value considered here. Allowing for the uncertainties in gas temperature, velocity dispersion, etc., the minimum value for which the photoionization models work well could probably be lowered by a factor of $\sim$2, so that if photoionization is the explanation of the H I cutoff, then $5 \times 10^3 \lesssim \phi_{i,\rm ex} \lesssim 5 \times 10^4$ photons cm^{-2} s^{-1}. (Note that this is the one-sided, normally incident photon flux.) Bochkarev & Sunyaev (1977) obtained very similar values for $\phi_{i,\rm ex}$; assuming a flat spectral distribution for the background between 13.6 and 124 eV, they estimated $\phi_{i,\rm ex}$ from comparison with H I observations of M31, finding $\phi_{i,\rm ex} \sim 0.5$–5×10^4 photons cm^{-2} s^{-1}.

There are a number of factors that make the estimate of the ionizing photon flux somewhat uncertain. In addition to temperature variations, uncertainty is introduced by the unknown density structure within the gas. In the calculations in this paper it has been assumed that the gas is smoothly distributed (§ 3). In fact, the good agreement between the models and the NGC 3198 data imply this assumption must be correct; if most of the mass of the neutral interstellar medium were clumped into clouds, with a large density enhancement with respect to the mean density, then photoionization models would not explain the cutoff. The greatly increased recombination rate in the clouds would keep them largely neutral to much lower column densities, and it would be necessary to invoke a rather sudden change in cloud properties with radius to explain the sharp edge seen in NGC 3198 and M33.

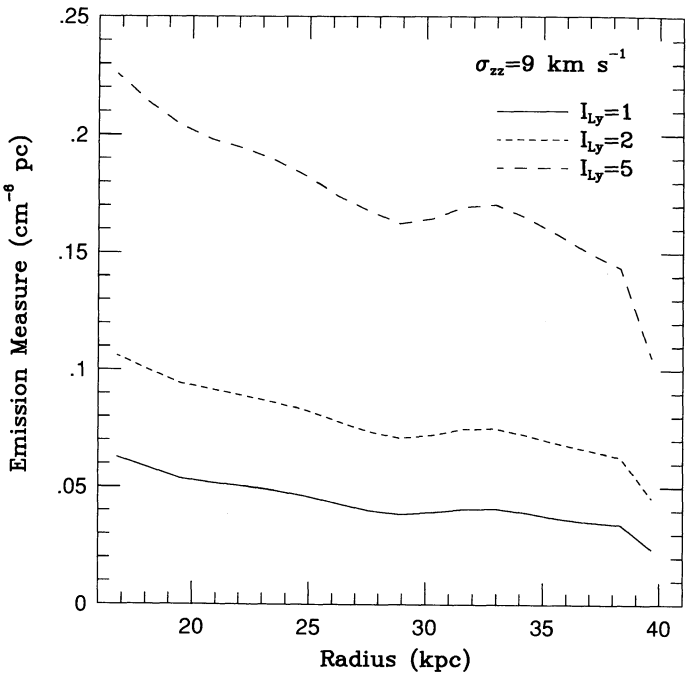

FIG. 14.—The emission measure of the ionized gas (in cm^{-6} pc) for the NGC 3198 models of the SW major axis, for $\sigma_{zz} = 9$ km s^{-1} and $I_{\rm Ly} = 1$, 2, and 5.

However, it is possible that density enhancements at some scale do exist within the gas. While such clumping would simplistically require an ionizing photon flux higher by a factor of $n_{\rm cl}/\bar{n}$ (where $n_{\rm cl}$ is the clump density and $\bar{n}$ is the mean gas density) in a homogeneous medium to produce the same neutral column density as in the uniformly distributed case, this is not true here because of the nonuniformity of the medium. The required ionizing photon flux will depend on the column density scale of the clumps as well as their density.

One way of discriminating between clumped and nonclumped models and between different values of the ionizing photon flux is to determine the emission measure of the ionized gas. Figure 14 shows the emission measure as a function of radius for a set of NGC 3198 models, for $\sigma_{zz} = 9$ km s^{-1} and three values of $I_{\rm Ly}$. The emission measures at column densities above $N_{\rm cr}$ differ by about a factor of 4 between the $I_{\rm Ly} = 1$ and $I_{\rm Ly} = 5$ models. The emission measures would be larger for $N_{\rm H}^{\rm tot} < N_{\rm cr}$ if the gas is in fact clumpy. Unfortunately, the emission measures are too small (by about an order of magnitude) to be detected with current instrumental sensitivities. Detections or stringent upper limits to the emission measures would provide an upper bound to the extragalactic ionizing photon flux without any of the complications present in studies of the high-velocity clouds, such as distance uncertainties and the amount of leakage of UV photons from sources in the disk.

The values for the extragalactic ionizing flux required to explain the sharp edge seen in NGC 3198 are consistent with previous upper limits. With additional observational constraints on the neutral gas velocity dispersion and the emission measure of ionized gas for NGC 3198 and other galaxies, it will be possible to considerably improve the current estimate of $\phi_{i,\rm ex}$ and make an indirect but relatively model-independent

determination of this cosmologically important quantity. Comparison of this $z = 0$ value for the ionizing background with determinations at higher redshift (e.g., Batlijk, Duncan, & Ostriker 1988) will place constraints on the nature and evolution of the sources of ionizing photons.

6.3. *Implications*

The abrupt edges to neutral hydrogen disks produced by the extragalactic radiation field have very unfortunate consequences for studies of galaxy dynamics. Since the cutoff column density varies little with galaxy parameters, it will be impossible to measure galaxy rotation curves at column densities below $N_{cr} \sim$ a few times 10^{19} cm^{-2}. The sharp decline in the neutral gas fraction severely limits the utility of the 21 cm line at column densities $N_H^{tot} < N_{cr}$. Furthermore, the emission measure of the ionized gas is at present unobservably small, so that observations of optical recombination lines such as Hα are also unfeasible. It is perhaps a matter of viewpoint whether this restriction is outweighed by the constraints on the extragalactic ionizing flux that modeling of these sharp edges provides.

Ionization of gas by the extragalactic background also implies that there may be a population of galaxies and/or intergalactic clouds which are undetectable in the 21 cm line. There are fairly stringent limits on populations of low-luminosity gas-rich dwarf galaxies or low-surface brightness galaxies from 21 cm surveys (Briggs 1990; Weinberg et al. 1991). Galaxies (or gas clouds) with average gas surface densities $N_H^{tot} \lesssim N_{cr}$ will be mostly ionized, and such objects will be effectively invisible in the 21 cm line. As can be seen in Figure 11, N_{cr} is a decreasing function of halo surface density, with $N_{cr} \propto \Sigma_h^{0.55-0.65}$, the exact exponent depending weakly on the galaxy model and on I_{Ly}. (This differs slightly from the analytic results of § 4 because of the varying importance of self-gravity as the gas column density decreases, and because the relative accuracy of the approximation used for σ_h is a function of radius.) Thus low-mass or low surface-density galaxies will have larger values of N_{cr} and will remain mostly ionized at larger total gas column densities. The amount of mass that could be present in such objects will depend on how they are dynamically supported (i.e., rotational or random motions), since this will determine both the surface densities and the local volume densities for a given mass.

In addition, if, as suggested here, the sharp edges are ionization edges rather than physical truncations of the gas in the galactic potential, we don't actually know how large the gaseous disks of galaxies are. Substantial column densities of ionized gas may extend to much larger radii than seen in 21 cm observations, and the small neutral fractions in these columns may be sufficient to produce observable Lyα absorption. This has important implications for QSO absorption-line systems. Application to the low-redshift Lyα absorption lines seen toward 3C 273 are discussed in Maloney (1992).

The success of the photoionization models in explaining the NGC 3198 observations suggests that the assumed physical conditions, namely, an interstellar medium outside the optical disks of galaxies that is warm and smoothly distributed, rather than cloudy, is correct. The low interstellar pressures at these radii will preclude the existence of cold clouds as a stable pressure-equilibrium phase, so this is perhaps not surprising. However, this could be either the primordial state of the gas, or the result of time-dependent heating and ionization of the gas. Most models for the behavior of the extragalactic radiation field (e.g., Miralda-Escudé & Ostriker 1990, and references therein) produce an increase of one or two orders of magnitude in the ionizing photon flux between the present and $z \sim 1$–2. Thus it is possible that the gas at these large radii was originally in clouds that were photoionized and photoevaporated by the extragalactic radiation field at an earlier time.

The time-dependence of the background ionizing flux also raises interesting questions regarding the damped Lyα systems. With photoionizing fluxes 10 or 100 times larger than the present-day value at $z \sim 2$, the critical column density for the gas to be significantly neutral would be $N_c \sim 10^{20}$–10^{21} cm^{-2}. Exactly what this will mean for the interpretation of the damped Lyα systems will depend not only on the time dependence of the ionizing photon flux, but also on how the gas column density as a function of radius in these systems has evolved.

7. SUMMARY

The results presented here show that the very sharp truncation of the neutral hydrogen distribution seen in NGC 3198 (and probably M33) is well modeled as the result of ionization of the atomic gas by the extragalactic radiation field. Below a critical column density $N_c \sim$ a few times 10^{19} cm^{-2} the gas is dominantly ionized and undetectable in the 21 cm line. The photoionization models imply that the total (neutral plus ionized) disk gas distribution in NGC 3198 is actually fairly axisymmetric. The critical column density for ionization is not a strong function of galaxy mass or mass distribution; thus *all galaxies should show a cutoff at approximately the same column density*. This effect places an unfortunate limit on the usefulness of the 21 cm line for measuring rotation curves at low column densities. However, it also makes it possible to estimate the extragalactic ionizing photon flux. Specific models of NGC 3198 suggest that this flux $5 \times 10^3 \lesssim \phi_{i,ex} \lesssim 5 \times 10^4$ photons cm^{-2} s^{-1}. Observational constraints on the emission measures interior to the cutoff radius and on the velocity dispersion of the neutral gas will allow a more precise estimate of the extragalactic ionizing photon flux. These results are in good agreement with the prescient paper of Bochkarev & Sunyaev (1977), who predicted that such cutoffs would be common in disk galaxies, and have important implications for QSO absorption-line systems.

Much of this work was done while I had the pleasure of holding a postdoctoral fellowship at the Sterrewacht Leiden, funded by the Nederlandse Organisatie voor Wetenschappelijk Onderzoek (NWO) under grant No. 782-372-025. It was completed while I was supported by the National Academy of Sciences through an NRC postdoctoral fellowship, and by the NASA Astrophysical Theory Program at the University of Colorado under grant NAGW-766. I have greatly benefited from discussions with J. Dickey, R. Sancisi, J. van Gorkom, R. Reynolds, P. Sackett, F. Briggs, S. Casertano, V. Icke, M. Fall, D. Hollenbach, L. Danly, M. Dopita, and L. Sparke. I am very grateful to J. van Gorkom for providing data in advance of publication. X. Tielens, J. Black and especially D. Hollenbach provided valuable comments on a draft of this paper. R. Reynolds brought the high-velocity cloud study of Cohen (1982) to my attention. M. van Steenberg generously provided me with his secondary-electron code. I would especially like to thank J. Dickey for prodding me to take this idea seriously.

REFERENCES

Bajtlik, S., Duncan, R. D., & Ostriker, J. P. 1988, ApJ, 327, 570
Begeman, K. 1989, A&A, 223, 47
Binney, J., & Tremaine, S. 1987, Galactic Dynamics (Princeton Univ. Press)
Bochkarev, N. G., & Sunyaev, R. A. 1977, AZh, 54, 957 (trans. in Soviet Astr., 21, 542)
Bosma, A. 1981, AJ, 86, 1825
Briggs, F. H. 1990, AJ, 100, 999
Briggs, F. H., Wolfe, A. M., Krumm, N., & Salpeter, E. E. 1980, ApJ, 238, 510
Carignan, C., & Beaulieu, S. 1989, ApJ, 347, 760
Carignan, C., Charbonneau, P., Boulanger, F., & Viallefond, F. 1990, A&A, 234, 43
Cohen, R. J. 1982, MNRAS, 200, 391
Corbelli, E., Schneider, S. E., & Salpeter, E. E. 1989, AJ, 97, 390
Dickey, J. M., Hanson, M. M., & Helou, G. 1990, ApJ, 352, 522
Donahue, M., & Shull, J. M. 1991, ApJ, 383, 511
Elitzur, M., & Netzer, H. 1985, ApJ, 291, 464
Felten, J. E., & Bergeron, J. 1969, ApL, 4, 155
Fransson, C., & Chevalier, R. A. 1985, ApJ, 296, 35
Hill, J. K. 1974, A&A, 34, 431
Hummer, D. G., & Seaton, M. J. 1964, MNRAS, 127, 217
Kuijken, K., & Gilmore, G. 1989, MNRAS, 239, 571
Kulkarni, S. R., & Fich, M. 1985, ApJ, 289, 792
Kutyrev, A. S., & Reynolds, R. J. 1989, ApJ, 344, L9
Lake, G., & Feinswog, L. 1989, AJ, 98, 166
Lockman, F. J., & Gehman, C. S. 1991, ApJ, 382, 182
Maloney, P. 1990, in The Interstellar Medium in Galaxies: Contributed Papers, ed. D. J. Hollenbach & H. A. Thronson, Jr. (NASA CP 3084), 1
———. 1992, ApJ, 398, L89
———. 1993, in preparation
Mather, J. C., et al. 1990, ApJ, 354, L37
Miralda-Escudé, J., & Ostriker, J. P. 1990, ApJ, 350, 1
Osterbrock, D. E. 1988, Astrophysics of Gaseous Nebulae and Active Galactic Nuclei (Mill Valley, CA: University Science Books)
Reynolds, R. J. 1987, ApJ, 323, 553
Reynolds, R. J., Magee, K., Roesler, F. L., Scherb, V., & Harlander, J. 1986, ApJ, 309, L9
Sackett, P. D., & Sparkle, L. S. 1990, ApJ, 361, 408
Sancisi, R. 1987, in QSO Absorption Lines, ed. J. C. Blades, D. A. Turnshek, & C. A. Norman (Cambridge Univ. Press), 241
Sargent, W. L. W., Young, P. J., Boksenberg, A., Carswell, R. F., & Whelan, J. A. J. 1979, ApJ, 230, 49
Schwartz, D. A. 1979, in Proc. 21st Cospar Symp., X-Ray Astronomy, ed. W. A. Baity & L. E. Peterson (Oxford: Pergamon), 453
Shostak, G. S., & van der Kruit, P. C. 1984, A&A, 132, 20
Shull, J. M., & van Steenberg, M. E. 1985, ApJ, 298, 268
Silk, J. 1971, A&A, 12, 421
Silk, J., & Sunyaev, R. A. 1976, Nature, 260, 508
Songaila, A., Bryant, W., & Cowie, L. L. 1989, ApJ, 345, L71
Stocke, J. T., Case, J., Donahue, M., Shull, J. M., & Snow, T. P. 1991, ApJ, 374, 72
Sunyaev, R. A. 1969, ApL, 3, 33
van Albada, T. S., Bahcall, J. N., Begeman, K., & Sancisi, R. 1985, ApJ, 295, 305
van Gorkom, J. H. 1991, in Atoms, Ions and Molecules: New Results in Spectral Line Astrophysics, ed. A. D. Haschick & P. T. P. Ho (San Francisco: ASP)
van Gorkom, J. H., Cornwell, T., van Albada, T. S., & Sancisi, R. 1993, in preparation
van der Kruit, P. C. 1988, A&A, 192, 127
van der Kruit, P. C., & Shostak, G. S. 1982, A&A, 105, 351
Weinberg, D. H., Szomoru, A., Guhathakurta, P., & van Gorkom, J. H. 1991, ApJ, 372, L13
Wevers, B. M. H. R. 1984, Ph.D. thesis, Rijksuniversiteit Groningen
Whitmore, B. C., McElroy, D. B., & Schweizer, F. 1987, ApJ, 314, 439
Williams, R. E. 1967, ApJ, 147, 556